sustainability

MDPI

Article

Derivation of Coastal Erosion Susceptibility and Socio-Economic Vulnerability Models for Sustainable Coastal Management in Senegal

Cheikh Omar Tidjani Cissé [1], Ivan Marić [2,*], Fran Domazetović [2], Katarina Glavačević [3] and Rafael Almar [4]

[1] Laboratory of Dynamics and Integrated Management of Coastal Areas, University of Quebec in Rimouski, 300 Ursuline Path, P.O. Box 3300, Rimouski, QC G5L 3A1, Canada; cheikhomartidjani.cisse@uqar.ca
[2] Center for Geospatial Technologies, Department of Geography, University of Zadar, 23000 Zadar, Croatia; fdomazeto@unizd.hr
[3] Independent Researcher, 67059 Ludwigshafen am Rhein, Germany; katarina.glavacevic@gmail.com
[4] Laboratory of Geophysical and Oceanographic Spatial Studies, University of Toulouse, 31013 Toulouse, France; rafael.almar@ird.fr
* Correspondence: imaric1@unizd.hr

Abstract: Coastal erosion has posed significant challenges to sustainability and socio-economic stability along Senegal's coastline, leading to substantial infrastructure losses. Using GIS multi-criteria decision analysis (MCDA), two sub-indices were derived for Senegal's coastal departments: the physical susceptibility (PSI) and the social-economic vulnerability (SVI) to coastal erosion. The integrated coastal erosion vulnerability (ICER) model was derived by their aggregation. A total of 26 criteria were used, 18 for PSI and 8 for SVI. The criteria weighting coefficients of the sub-indices were determined using the analytic hierarchy process (AHP). Validation of the model accuracy was performed using receiver operating characteristic (ROC) curves that were calculated based on a created coastal erosion cadaster and true positive (TP) sites and manually acquired true negative (TN) sites. The accuracy assessment confirmed the consistency of the physical susceptibility model (PSI) and proved that existing coastal erosion sites are within (5) very high susceptibility areas. Through the generated ICER, the coastal departments were divided into areas of (1) very low, (2) low, (3) medium, (4) high and (5) very high vulnerability to coastal erosion. Very high (5) and high (4) classes cover around 31% of the coastal departments, mostly encompassing a narrow coastal strip and low river valleys and mouths. The presented coastal susceptibility and vulnerability maps, with a spatial resolution of 30 m, identified problematic areas in Senegal's coastal departments and can help decision-makers in the construction of effective coastal zone management and sustainable development.

Keywords: coastal erosion; susceptibility; socio-economic vulnerability; sustainability; Senegal

Citation: Cissé, C.O.T.; Marić, I.; Domazetović, F.; Glavačević, K.; Almar, R. Derivation of Coastal Erosion Susceptibility and Socio-Economic Vulnerability Models for Sustainable Coastal Management in Senegal. *Sustainability* **2024**, *16*, 7422. https://doi.org/10.3390/su16177422

Academic Editor: Giorgio Anfuso

Received: 9 July 2024
Revised: 23 August 2024
Accepted: 23 August 2024
Published: 28 August 2024

1. Introduction

Coastal zones are unique and dynamic environments that are increasingly anthropized and inhabited due to their socio-economic importance [1]. Sandy beaches account for around 31% of all coastal zones in the world [2]. They play a vital role for the population, providing essential ecosystem services that form a significant part of the economic base of many countries [3]. This has led to rapid urbanization, resulting in the occurrence of several environmental problems, most notably coastal erosion. Coastal erosion is a complex phenomenon that represents a significant risk [4]. It leads to the loss of coastline, causing the destruction of coastal ecosystems and human settlements along low-lying sandy areas [5]. Coastal erosion not only jeopardizes coastal stability but also leads to the occasional loss of natural habitats [3]. As the climate changes, this erosive trend is likely to intensify [6]. Rising sea levels and the frequency of extreme meteorological events will increase the vulnerability of coastal areas [7,8]. Among these, sandy coasts will be the most exposed.

The trend of retreating coastlines is a global phenomenon. Indeed, 70% of the world's sandy coasts are affected by erosion [9] and, in some cases, the eroded sandy coastline represents 60–90% of the total coastline [9]. Erosive dynamics can be explained by both natural and anthropogenic factors [10]. Almost 20% of the coastline of the European Union (EU) is affected by coastal erosion [11]. In the United States, 66% of the coastline of the Gulf of Mexico is affected by erosion [12]. In Latin America, coastal zones face pressing challenges, highlighting coastal erosion as a major concern. In Southeast (SE) Asia, coastal erosion is often mentioned as a coastal flooding hazard. Some SE Asian countries (e.g., Bangladesh) and the Maldives are threatened with the loss of landmass due to the high rate of coastal retreat. China's most developed coastal city, Shanghai, is heavily threatened by coastal erosion [13].

Coastal areas in Africa are particularly exposed [14,15]. It is the continent with the highest presence of sandy beaches (66%) [2], making it particularly exposed to sea-related risks [16]. This vulnerability is catalyzed by heavy urbanization and insufficient coastal protection structures [17]. In North Africa, coastal erosion poses a real threat to large urban areas due to rising sea levels. North Africa, particularly the Maghreb, is the second most affected region in terms of coastal erosion, after Southeast Asia [18]. In West Africa, coastal erosion is a major challenge to regional development, responsible for the rapid loss of land and property [15,17,19,20]. For the 4400 km of coastline from Senegal to Sierra Leone, the average rate of coastline retreat is 1.2 to 6 m/year, and from Cote d'Ivoire to Nigeria, the values vary from 1 to 15 m/year [21]. This constitutes one of the greatest threats to the socio-economic and environmental balances of countries south of the Sahara, particularly the cities along the Atlantic seaboard [22] (p. 2). It is one of the regions of the world whose coastlines and deltaic zones are most exposed to coastal erosion linked to rising sea levels and heavy urbanization [23]. From the coasts of the West to those of Central Africa, the coastal erosion has been intensifying for over four decades [2,24–26]. Coastal retreat in West and Central Africa is the result of natural, anthropogenic or combined factors [24,27,28]. This is likely to be aggravated by climatic projections leading to a rise in the sea level and an increase in the frequency and intensity of storms [29]. Projections of the sea-level rise [30] by 2100 suggest that this could be accompanied by an intensification and recurrence of cyclones. Rising sea levels will influence bathymetric surf in coastal areas, leading to stronger swell conditions at the coast [31]. Many West African coastal cities are not prepared for coastal hazards [23].

With over 700 km of mainly sandy coastline, the Senegalese low-lying coast is showing signs of increased vulnerability to erosion. The sections of coastline most affected by coastal erosion are Dakar, Mbour, Saint-Louis and Ziguinchor [32–35]. Coastal erosion is a problem of varying intensity along Senegal's coasts, with the cities of Saint-Louis and Rufisque being the most exposed [36]. Senegal's coasts have undergone significant morphological changes in recent years [32]. The rates of coastline retreat observed oscillate between 1 and 2 m/year [37]. In the worst-affected areas, the coastline is retreating at an average rate of 2 m/year [33]. Coastal erosion occurs almost everywhere on the Senegalese coast, but with different proportions depending on the causes and the environmental characteristics [38]. Therefore, erosion is a real economic threat [39]. In the Mbao Bargny section, coastline retreat is estimated at 1 m/year [32]. In the Djiffere sector, the rate reached 3.83 m between 1989 and 2013 [40]. As the Petite Côte is highly urbanized, this erosion undoubtedly impacts socio-economic activities [36]. In Senegal, coastal erosion is one of the biggest environmental problems facing the southern coastline, particularly the Petite Côte. The situation has become alarming in many places on the south coast of Dakar [34,41]. Although some drivers of this phenomenon are in part of social origin (e.g., coastal development, beach sand mining), combined with natural problems (e.g., slope instability, sediment deficit), their effects are expected to be enhanced by climate change [42]. Protective structures are present along the Rufisque coastline from Mbao to Bata. Today, this part of the Senegalese coastline is the most artificialized, with the largest representation of protective structures [43]. This artificialization is the result of the vulnerability recognized

by populations exposed to the risks of erosion [44]. Although protective structures have been built to limit the coastal erosion, studies carried out on the Senegalese coast show that these structures only partially play the role of ramparts [35,43,45,46].

Although most sections of Senegal's coastline are subject to coastal erosion, few parts of Senegal's coastal zones have been the subject of a comprehensive susceptibility [47,48] and vulnerability assessment. In order to determine the presence and spatial distribution of coastal erosion on the coast of Senegal, the main objective of this study is to derive an integrated coastal erosion vulnerability (ICER) model using the GIS multi-criteria decision analysis (MCDA) approach. Vulnerability has been extensively used in hazard studies. However, it lacks a universal definition [49]. It refers to the degree to which a system, community, or asset is likely to experience damage when exposed to a specific hazard. It can include a wide range of factors [50]. Susceptibility is a narrower concept that refers to the inherent characteristics of an area or object that make it more likely to be affected by a specific hazard. It focuses more on the physical properties that determine how easily something can be impacted [47]. Regarding the erosion hazard, assessment of areas potentially susceptible to the occurrence of coastline retreat or gully erosion is essential for the determination of the most vulnerable areas (social context) and for planning measures for the mitigation of their negative effects [47]. Coastal vulnerability to specific hazards has been analyzed using various methodologies [51]. One of the most popular methods is the coastal vulnerability index (CVI) defined in [52]. A large number of index variations are proposed. A good review is provided in [53], highlighting vulnerability indices derived based on physical, socio-economic parameters and those combined. Namely, the CVI only considers the physical aspects of coastal vulnerability. A suitable coastal vulnerability index should incorporate the socio-economic aspect [51,54]. In most of the studies of physical susceptibility to coastal erosion, social vulnerability related to socio-economic factors is not included [55].

Following this, in our research, two sub-indices have been developed: the physical susceptibility (PSI) and the socio-economic vulnerability (SVI) to coastal erosion models. By combining these two sub-indices, we produced an integrated coastal erosion vulnerability model (ICER). It is seen as the combination of the physical and social aspects of a coastal departments of Senegal and it is location-specific. The concept of vulnerability combines elements from physical and social aspects that make a particular system vulnerable to experiencing socio-economic loss from natural hazards.

Although in the derivation of these models most authors use GIS-MCDA, this methodology has been improved by using a large number of criteria acquired from open-source data (OSM) and dividing integrated vulnerability model in two sub-indices.

Study Area

Senegal is a West African developing country, which highly relies on a 731 km long coastline characterized by a variety of habitats, ranging from floodplain depressions and salt flats to the volcanic outcrop that stands out along the otherwise sandy coastline. The continental shelf, bounded by a 200 m isobath, covers around 28,700 km^2 [42]. The Senegalese coastline is an environment of great diversity. Its ecological wealth makes it a provider of ecosystem services. It offers cultural and social supply and economic benefits [56]. According to CSE State of the Environment Report [57], the coast is home to 90% of the country's industries and contributes 68% of the country's gross domestic product (GDP). A significant proportion of Senegal's population lives close to the coast, concentrated in the country's largest urban centers [58]. The Senegalese coast is characterized by a high concentration of people, representing 60% of the country's population in 2010 [39]. One of the most populous regions is the Saloum Delta, with around 16% of total country's population (Figure 1).

Figure 1. Geographical location of Senegal within Africa (**A**); location of the study area (coastal departments) and five geomorphological coastal entities within Senegal (SSD—Siné-Saloum Delta) (**B**).

The Senegal coastal zone stretches to the southern tip of Diembéring. It is structured around the Cape Verde peninsula and the three river mouths of the Senegal, Siné-Saloum and Casamance rivers. These hydrological entities constitute geomorphological discontinuities in the coastline [59]. Overall, the coastal zone corresponds to the western limit of the Meso-Cenozoic Senegal–Mauritania sedimentary basin. Geologically, it is characterized by great sedimentary thicknesses (6000 m or more east of Dakar) and a faulted structure, very present between Dakar and Mbour, where the coast is cut into a succession of horsts and grabens [60,61]. The intense volcanism of the Oligo-Miocene to Quaternary age is well represented on the Cape Verde peninsula.

A volcanic basement forming the Cape Verde peninsula divides the Senegalese coastline into two distinct blocks: the Petite and Grande Côte [59]. This volcanic basement has played a role in the morphological configuration of Senegal's coasts. It is responsible for a major change in the direction of the coastline, isolating the Petite and Grande Côte [59]. The Petite Côte lies south of the Cape Verde peninsula and extends as far as the mouth of the Siné-Saloum. The Senegalese coast can be divided into five geomorphological entities:

(1) The Senegal River Delta, home to the Djoudj wetland, as far as the Mauritanian coast, diverted to the south by the Langue de Barbarie [62];

(2) The Grande Côte or Côte Nord (from Yoff to Saint-Louis) is marked by a broad dune massif backed by wet depressions known as Niayes. They constitute an environment with dunes and depressions often flooded by the outcrop of the water table [63]. Backed by dune massifs, the Grande Côte is predominantly influenced by north-westerly swells, which induce a southward littoral drift. Sediment estimates parallel to the coast vary from 200,000 to 1,500,000 m^3/year [37,60];

(3) The Petite Côte is a sandy–rocky coast alternating between small rocky outcrops and sandy bays with a few lagoons. The Petite Côte lies to the south of the Dakar peninsula. The coast is more indented, with rocky and sandy types [64]. It is subject to the action of north-westerly swells, the energy of which is dissipated by the refraction phenomena observed around the Cape Verde peninsula. In contrast to the Grande Côte, the sediment input from the southeast drift is low, at 10,500 to 300,000 m^3 [60];

(4) The Siné-Saloum Delta is characterized by a marshy shoreline, bordered by mangroves at river mouths;

(5) Casamance is a sandy coastline backed by a fluviomarine complex that also features mangrove swamps [62].

Senegal's climate is characterized by two distinct seasons, the dry season from October to May and the rainy season from June to September. The climate is influenced by the country's tropical latitude and the seasonal movement of the intertropical convergence zone (ITCZ). The dominant winds in Senegal are dry winds originating from the continental interior and moist maritime winds, from the west and northwest, responsible for rainfall [65]. During the monsoon season, from July to October, most dominant are weak westerly winds. Then, the region receives its main annual precipitation [66]. The arid regions experience an annual precipitation of less than 300 mm/y, whereas the southern areas receive an average of 1200 mm/y. Senegal's average annual temperature from 1960 to 1990 was 27.8 °C, reaching monthly averages of up to 35 °C during the hottest seasons [67]. These factors contribute to the formation of three climate zones: coastal, Sahelian, and Sudanic. The coastal zone is situated along a narrow strip of the Atlantic coastline spanning approximately 16 km from Saint-Louis to Dakar. In response to globally increasing temperatures, the sea level off the coast of Senegal is projected to rise. Like many West African coasts, Senegal's coasts are marked by an information gap relating to the sea-level rise data. According to [68], even though the Dakar tide gauge station has the longest time series of tide gauge data in West Africa, it is characterized by a huge data gap. Apart from [69,70], there is no research on sea-level rise over the 700 km of Senegal's coastline. Moreover, [69,70] do not cover the entire Senegalese coastline. In view of this lack of data on the sea-level rise, it is difficult to provide an overall view of the trend in the sea-level rise, particularly along the entire Senegalese coastline. Using in situ data from the Dakar tide gauge and spatial altimetry over a long time sequence, [69] indicates that the sea-level rise trend in the Cape Verde peninsula is estimated at 2.24 mm/year. However, a recent paper on sea-level rise trends in Senegal, Cape Verde and Mauritania reveals that over 1993–2018, the sea-level rise trend is estimated at 1.52 mm/year [70]. Winters in this zone are characterized by mild temperatures, with January minimums of around 17 °C, while the maximum temperatures in May typically do not surpass 27 °C. Rainfall commences in June, peaks in August, and concludes in October, with an average annual precipitation of about 500 mm [65].

2. Materials and Methods

Derivation of the integrated coastal erosion vulnerability model (ICER) was conceptualized through the application of the GIS-MCDA workflow, which consisted of six steps (Figure 2).

In the first step (1), the main objective was defined. Considering that the socio-economic vulnerability model of coastal erosion is often not included in analyses, the first step defined two sub-indices, derivation of the physical susceptibility (PSI) and social-economic vulnerability (SVI) to coastal erosion models.

In the second step, determination of the predisposing criteria (2) for susceptibility and vulnerability modeling was performed according to the analyzed literature and considering the size of the study area (coastal departments of Senegal) and the available data. Constraints (Boolean) criteria were defined as departments that do not border the ocean. Each criterion was selected based on its direct relevance and impact on coastal erosion processes. The selected criteria encompass a broad range of physical (PSI) and socio-economic (SVI)

factors that influence coastal erosion and have effects on human communities and infrastructure. In Tables 1 and 3, an overview of the defined criteria is provided and examples in the literature are shown. The selection of criteria was supported by an extensive literature review. Previous studies on coastal erosion and vulnerability assessments in similar contexts guided the selection of criteria. With the inclusion of 18 criteria for the PSI and 8 criteria for the SVI, we ensured a comprehensive assessment that covered the dimensions of physical susceptibility and social vulnerability. This detailed selection helps in capturing the complex nature of coastal erosion impacts. The chosen criteria are adaptable to different geomorphological contexts due to their fundamental relevance to coastal processes. For instance, factors like land use and socio-economic conditions can be universally applied but are weighted differently based on local conditions.

Table 1. Selected criteria for derivation of the coastal erosion susceptibility model (PSI).

ID		Criteria	Authors	Data Source
1	Terrestrial	Elevation (E)	[71,72]	SRTM
2		Slope (S)	[72,73]	SRTM
3		Vertical Distance from Channel Network (VDCN)	[71]	SRTM + SAGA toolbox 9.5.1
4		Lithology (L)	[71]	GliM v1.0
5		Topographic Wetness Index (TWI)	[47,71,72,74]	SRTM + SAGA toolbox
6		Topographic Positioning Index (TPI)	[75]	SRTM + SAGA toolbox
7		Topographic Ruggedness Index (TRI)	[75]	SRTM + SAGA toolbox
8		Planar Curvature (PC)	[47,71,72,74]	SRTM + ArcMap 10.8.1
9		Aridity Index (AI)	[76]	CGIAR CSI [77]
10		Aspect (A)	[78]	SRTM + ArcMap 10.8.1
11		Normalized Difference Vegetation Index (NDVI)	[71]	Sentinel 2a + ArcMap 10.8.1
12		Precipitation (P)	[71,73]	WorldClim [79]
13		Wind Shelter Index (WSI)	[80]	SRTM + SAGA toolbox
14		Wind Exposition Index (WEI)	[80]	SRTM + SAGA toolbox
15	Marine	Mean Wind Fetch (MWF)	[81]	SRTM + Waves (2012)
16		Bathymetry (B)	[82]	GEBCO [83]
17		Mean Wind Speed (MWS)	[84]	Global Wind Atlas [85]
18		Significant Wave Height (SWH)	[81]	Copernicus Data Marine [86]

The standardization was carried out in the third step (3), where the defined criteria were standardized to the same scale. In the fourth step (4), weight coefficients were determined using the AHP.

Then, in the fifth step (5), aggregation of the selected criteria was performed to produce the physical susceptibility (PSI) and social-economic vulnerability (SVI) models. Finally, these models were aggregated into the integrated coastal erosion vulnerability model (ICER). In the last (6) step, the accuracy and quality of the PSI model were validated using the ROC curves created based on the true positive (TP) sites from the created coastal erosion cadaster and the manually collected true negative (TN) sites.

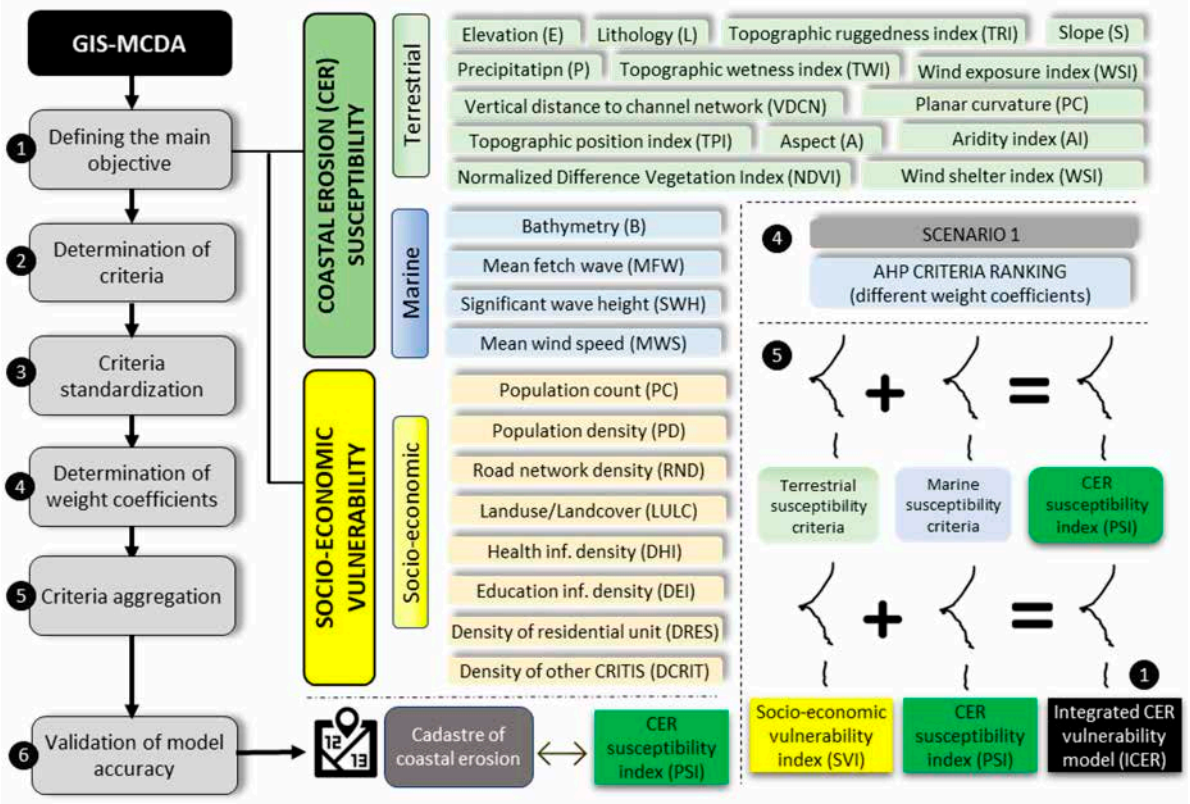

Figure 2. Methodological workflow of the integrated vulnerability model for coastal erosion (ICER).

2.1. Selection of Physical Susceptibility Criteria

In deriving a physical susceptibility (PSI) model, eighteen criteria were selected (Table 1). The criteria are divided into two groups: terrestrial and marine. Given that the raster models of terrestrial criteria represent "land" and the models of marine criteria represent "sea" (from coast to the ocean), it was necessary to find a way to merge them into a final model of physical susceptibility (PSI) that should encompass departments bordering the sea (from coast to interior land).

This was performed in such a way that the raster model of the terrestrial criteria (n = 14) was derived directly for departments bordering the sea, while the model of marine criteria (n = 4) was first derived as a coastline. This coastline was divided into vertex points with a distance of 30 m, where each vertex had an aggregated attribute of susceptibility (from 1–very low to 5–very high) to coastal erosion regarding the aggregated marine criteria. Then, these points were converted into polygons with the Create Thiessen polygons tool in ArcMap. However, given that the susceptibility to coastal erosion is being modeled, all the polygons further than 100 m from the coastline were automatically given the value of 1 (very low susceptibility), while the polygons closer to the coast (<100 m) kept the attributes of the vertices from which they were created. Then, the polygons were converted into a raster that represents the coastal erosion susceptibility model for marine criteria and encompasses the area of departments bordering the sea. The final PSI model was derived by aggregating the models of terrestrial criteria (n = 14) and marine criteria (n = 4) susceptibility to coastal erosion.

Although the criteria considered for deriving physical susceptibility are not exhaustive, they accurately represent predisposing factors for the occurrence of coastal erosion. All the selected criteria were acquired from open access (OA) sources (Table 1). These criteria are relevant for modeling the PSI to coastal erosion because they capture key environmental factors that influence erosion processes. The elevation (E), slope (S), and topographic ruggedness index (TRI) provide insights into the terrain's steepness and variability, which directly affect erosion rates. Factors like the lithology (L) and bathymetry (B) influence

the strength and composition of coastal materials. Indices such as the aridity index (AI) and precipitation (P) reflect climatic conditions that control erosion rates through water availability and the frequency of erosive events. Wind-related indices (WSI, WEI, MWS) and the significant wave height (SWH) indicate the energy and directionality of coastal processes, crucial for assessing erosion potential. Together with the vegetation indices (NDVI), these criteria offer a comprehensive framework for modeling coastal erosion susceptibility by integrating morphometric, climatic, and ecological variables. All the morphometric criteria were derived based on Shuttle Radar Topography Mission (SRTM), with a spatial resolution of 30 m.

- The elevation (E) is recognized as an important criterion since low-lying coastal areas are more prone to erosion due to the proximity to sea level.
- Although higher slope (S) values generally indicate higher susceptibility to coastal erosion, in this research, lower values were set as an indicator of higher susceptibility since this type of erosion prevails on the Senegal coast. Areas with lower slopes allow the penetration of water into the interior of the land. Lower slopes may facilitate the inland penetration of water during storm surges or high tide events. The (S) was generated using Slope tool in ArcMap 10.8.1.
- The vertical distance from channel network (VDCN) refers to the vertical position of a specific location relative to nearby channel networks. Locations with lower VDCN were considered more susceptible to erosion. This criterion was generated using the VDCN tool within SAGA toolbox.
- The lithology (L) is important in understanding the geological features of the coastal environment. Areas with resistant composition are less susceptible to erosion. These materials can withstand wave action and other erosive forces. Loose sediments contribute to higher erosion susceptibility and are more prone to being transported by waves and currents (Figure 3).
- The topographic wetness index (TWI) provides insights into the hydrological characteristics of the terrain, characterizing its potential relative wetness or moisture content. Since a higher TWI indicates the increased moisture content, this means that these areas are more prone to saturation, making them susceptible to coastal erosion.
- The topographic positioning index (TPI) provides the relative topographic position of the specific point as the difference between its elevation and the mean elevation of the user-defined neighborhood. Since a positive TPI generally indicates elevated positions, this value is considered less susceptible to coastal erosion.
- The topographic ruggedness index (TRI) quantifies the variability in elevation within a defined neighborhood, providing a measure of the roughness of a landscape. A higher TRI may indicate diverse topographic features, such as cliffs, rocky shorelines, or irregular coastal formations. Similar to the slope criteria, this parameter can influence coastal erosion susceptibility in two ways. However, given the specificity of coastal erosion in Senegal, lower values indicate increased susceptibility. The TWI, TPI and TRI criteria were generated using tools within the SAGA toolbox (Figure 3).
- The planar curvature (PC) characterizes the curvature of land, providing information about how the surface is shaped. Areas with concave curvature, forming depressions, are recognized as those susceptible to coastal erosion. This criterion was generated using the Curvature tool in Arc Map.
- The aridity index (AI) quantifies the dryness or aridity based on the balance between precipitation and potential evaporation. In coastal areas with a higher aridity index, the vegetation cover may be sparse and the soil may lack sufficient moisture. This can lead to reduced stability and increased vulnerability to erosion.
- The aspect (A) represents the exposure of the slope. Higher susceptibility values are given to those slopes that are exposed to the west side (Figure 3).
- The normalized difference vegetation index (NDVI) is widely used for quantifying the health and density of vegetation. Higher NDVI values are related to lower susceptibility to coastal erosion since they indicate denser and healthier vegetation. Cover

such as mangroves, seagrasses, or shrubs provides stabilizing effects, reducing the susceptibility to erosion. The NDVI was generated using the Image Analysis tool in ArcMap from Sentinel 2A imagery.

- The precipitation (P) can impact the susceptibility to coastal erosion since higher precipitation levels can cause increased runoff and the potential occurrence of water flow.
- The wind exposition index (WEI) criteria represent the average wind effect index for all directions using an angular step. Coastal areas with higher wind exposure are generally more susceptible to erosion. Winds from the ocean can result in stronger wave action, increased wind-driven erosion, and higher susceptibility to coastal retreat.

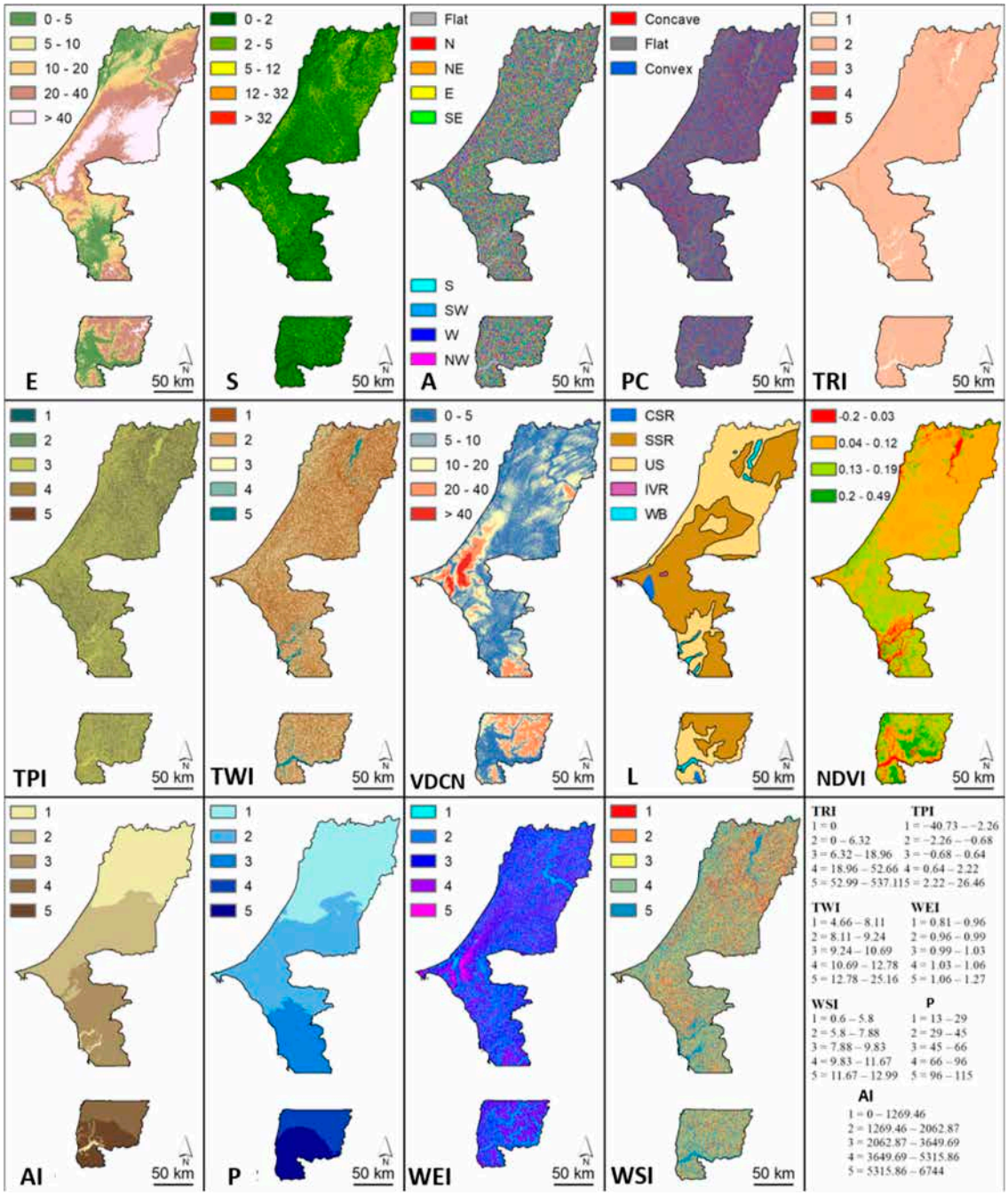

Figure 3. Selected terrestrial criteria for physical susceptibility (PSI) to coastal erosion.

- The wind shelter index (WSI) assesses the degree of wind protection provided by surrounding terrain. It is a dimensionless index where values below 1 indicate wind-

shadowed areas. The WSI has been generated using the SAGA toolbox. It was created as a weighting model of dominant winds that cause waves on the coast of Senegal (wind direction ranging from 180° to 0/360°). The weight coefficients of selected winds are calculated as their wind frequency percentage (Table 2). These data were used in the derivation of the mean wave fetch (MFW) criterion. Data from wind frequency rise used for the derivation of this model was downloaded from the [85] website (Figure 4).

Table 2. Direction of winds and calculated wind frequency used in the analysis.

Wind Frequency (%)	Frequency (%) of Selected Wind	Sector	Wind Direction (°)
1.0	1.7	6	180
3.0	0.5	7	210
7.0	11.7	8	240
15.0	25.0	9	270
15.0	25.0	10	300
10.0	16.7	11	330
9.0	15.0	12	360/0

- The mean wind fetch (MWF) refers to the distance over the water surface that wind travels to generate waves. It directly influences the energy and intensity of waves. Longer wind fetch distances allow waves to build up more energy as they travel across the water surface. This accumulated energy can result in more significant wave heights and greater erosive potential, leading to higher susceptibility to erosion. This criterion was generated using the Waves (2012) toolbox.

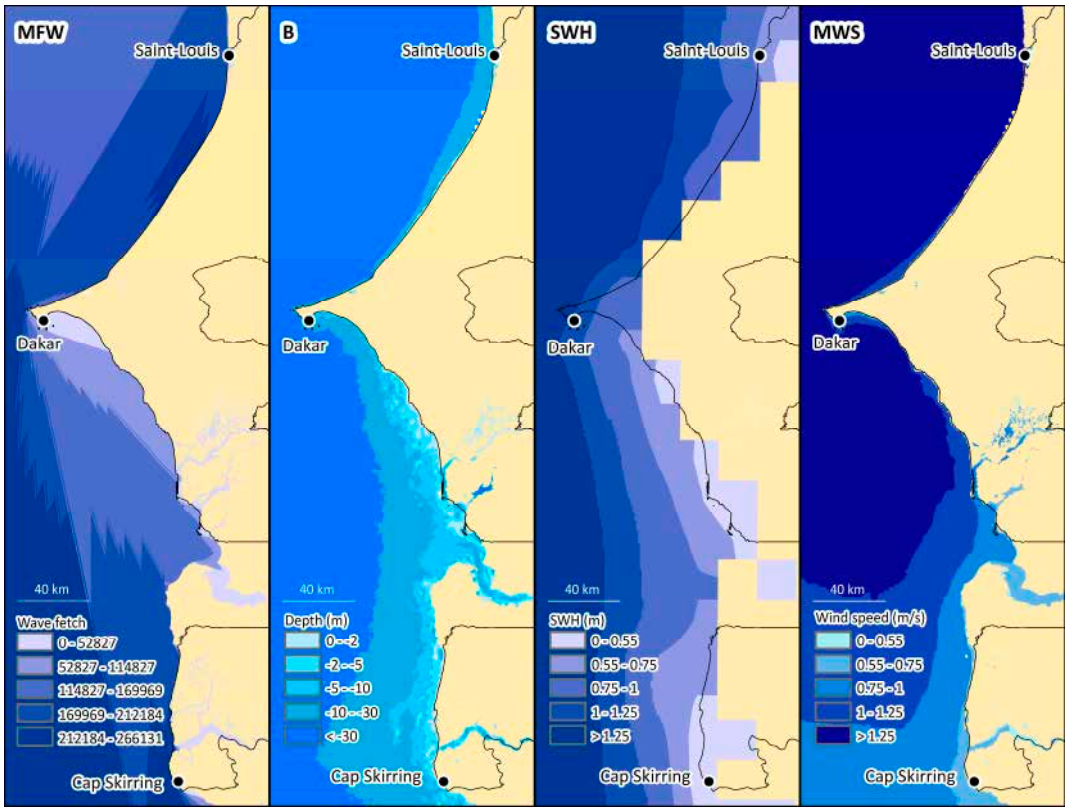

Figure 4. Selected marine criteria for physical susceptibility to coastal erosion.

- The bathymetry (B) can indirectly influence coastal erosion susceptibility. It impacts the transformation of waves as they approach the coastline. Shallower water depths cause waves to steepen and increase in height, amplifying their erosive power. Therefore, shallower bathymetry can lead to higher coastal erosion susceptibility due to the higher wave energy.
- The significant wave height (SWH) is a measure of the average height of the highest one-third of waves in a given area. It directly influences the erosive power of waves and their impact on coastal environments. Higher significant wave heights indicate more energetic waves capable of exerting greater force on the coastline, leading to increased erosion susceptibility (Figure 4).

2.2. Selection of Socio-Economic Vulnerability Criteria

Eight criteria were selected in deriving a socio-economic vulnerability model (SVI) for coastal erosion (Table 3). Although the criteria considered for social vulnerability are not exhaustive, they accurately represent social pressure in this study area. All the selected criteria were acquired from open access (OA) sources. The criteria used in the modeling of the (SVI) are selected such that they meet two requirements: (1) best represent the basic infrastructure/social element necessary for the functioning of the urban/rural system (population density, roads, hospitals, schools, other infrastructure, shops, etc.); and (2) are available as GIS data.

These criteria are relevant for SVI modeling of coastal erosion because they capture the essential human and infrastructural elements. The population count (PC) and population density (PD) indicate the number of people potentially affected by erosion. The densities of the road network (RND), health infrastructure (HID), educational infrastructure (EID), and other critical infrastructure (DCRIT) highlight the accessibility and availability of essential services. The density of residential units (DRES) provides insight into housing exposure. The land use and land cover (LU/LC) offer a comprehensive view of how land is utilized, reflecting the economic activities and ecological. Together, these criteria include the demographic, infrastructural, and land-use aspects necessary for an SVI assessment.

Table 3. Selected criteria for the social-economic vulnerability model (SVI).

ID	Criteria	Authors	Data Source
1	Population count (PC)	[87,88]	WordPop [89]
2	Population density (PD)	[73,87,88]	WordPop [89]
3	Density of road network (RND)	[88]	[90] + ArcMap Analysis
4	Density of health infrastructure (HID)	[91]	[90] + ArcMap Analysis
5	Density of educational infrastructure (EID)	[92]	[90] + ArcMap Analysis
6	Density of other critical infra. (DCRIT)	[93]	[90] + ArcMap Analysis
7	Density of residential units (DRES)	[73]	[90] + ArcMap Analysis
8	Land use/land cover (LU/LC)	[47,71–73,88,94]	ESA WorldCover [95]

- The PC and PD are fundamental criteria in assessing SVI. The coastal population concentration can significantly influence coastal erosion [87]. Larger populations and areas with higher population densities can face significant challenges in evacuation, resource distribution, and emergency response during coastal erosion events (Figure 5).
- The set of criteria regarding the RND, HID, EID, DRES and DCRIT were placed in such a way that higher values indicate higher vulnerability to coastal erosion, suggesting a greater concentration of population, infrastructure, and assets in areas that can be affected by coastal erosion [88].

All the criteria regarding the critical infrastructure were acquired from the *Geofabrik* website. Health infrastructure included *clinic*, *dentist*, *doctors*, *hospital*, *nursing home*,

pharmacy and *polyclinic* attributes. Educational infrastructure included *school*, *university*, kindergarten and *college* attributes, while other critical infrastructure included *mall*, *bank*, *post office*, *department store*, *marketplace*, *supermarket*, *food court* and *convenience store* attributes. All the raster density models (cell size = 30 m) were derived using the *Line Density* and *Kernel Density* tools within ArcMap. The search radius was set to 2000 m.

Although potential overlap occurs between the critical infrastructure criteria and the LU/LC, it was necessary to include the LU/LC as separate criteria in the analysis. The LU/LC provide a comprehensive overview of the general LU/LC classes across the Senegal coast. This broader perspective is essential for understanding the overall distribution of built-up areas, which includes but is not limited to critical infrastructure. The "Built-up" class captures all the urbanized and developed areas, encompassing residential, commercial, and other non-critical infrastructures. Also, this criterion indicates data about other classes that can have an important impact when modeling social vulnerability to coastal erosion (e.g., swamps, mangroves, etc.). Furthermore, while specific infrastructure data (e.g., density of health and educational facilities) are critical, they represent only a subset of the built environment, which does not have to be complete given that the OSM, i.e., Geofabrik is used as a data source

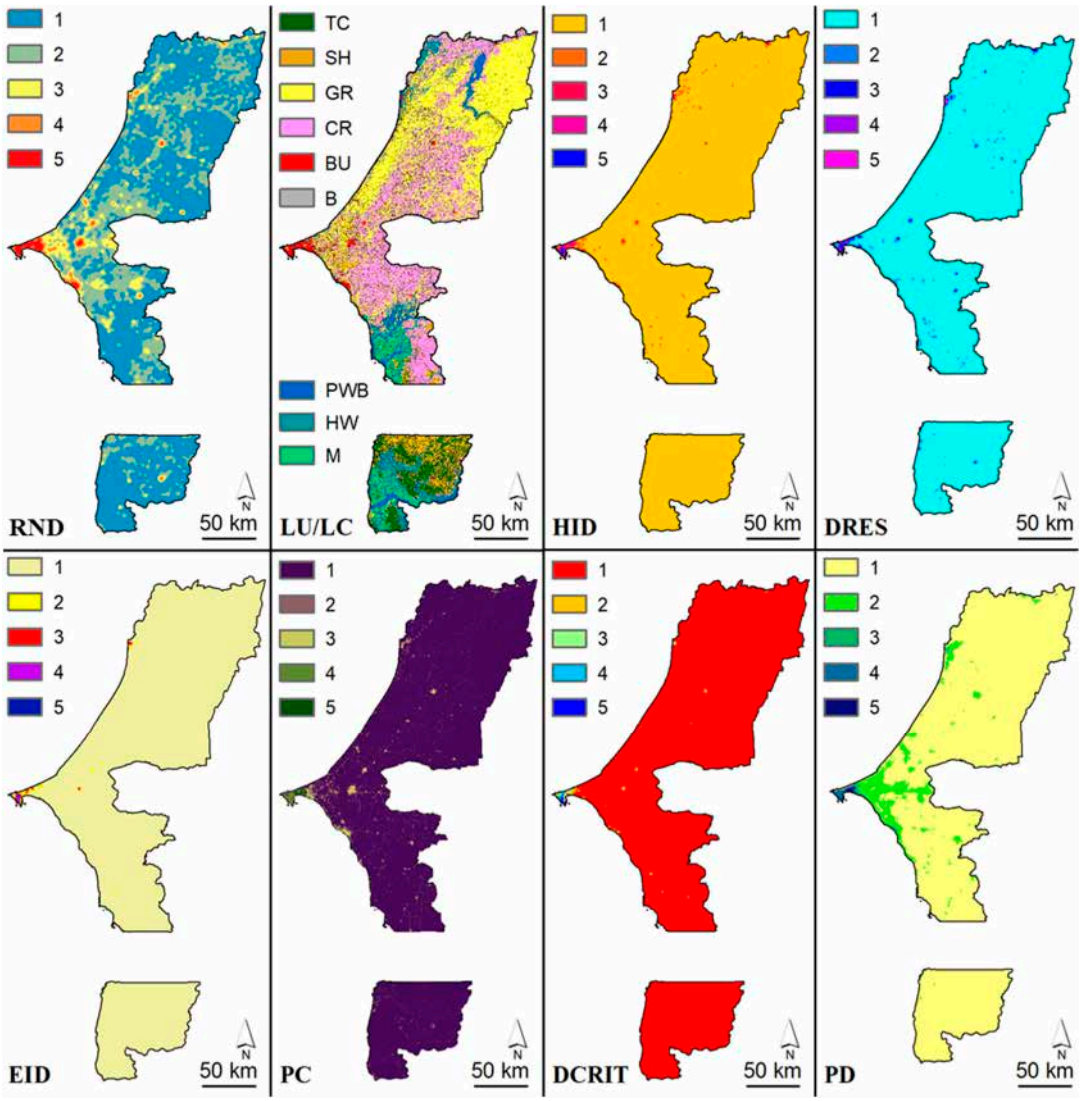

Figure 5. Selected criteria for socio-economic vulnerability to coastal erosion.

2.3. Criteria Standardization

Depending on the criterion type, the standardization was performed using the *decision-maker standardization* method and *Jenks* (*natural breaks*) classification method. The criteria are standardized on the same scale ranging from 1 to 5 (1—*very low*, 2—*low*, 3—*medium*, 4—*high*, 5—*extremely high*) (Table 4). When using diverse criteria for a specific GIS-MCDA model, it is justified to employ different standardization methods. This is because each criterion can vary in its nature and distribution, which requires the application of a specific standardization method. Using different standardization methods ensures that each criterion is transformed in a scale that best reflects its contribution to a specific phenomenon or process. As long as all the criteria are ultimately standardized on the same scale, from 1 (very low susceptibility) to 5 (very high susceptibility), the comparability and integration of standardized criteria are maintained. Figure 6 shows the standardized terrestrial criteria for physical susceptibility (PSI) to coastal erosion.

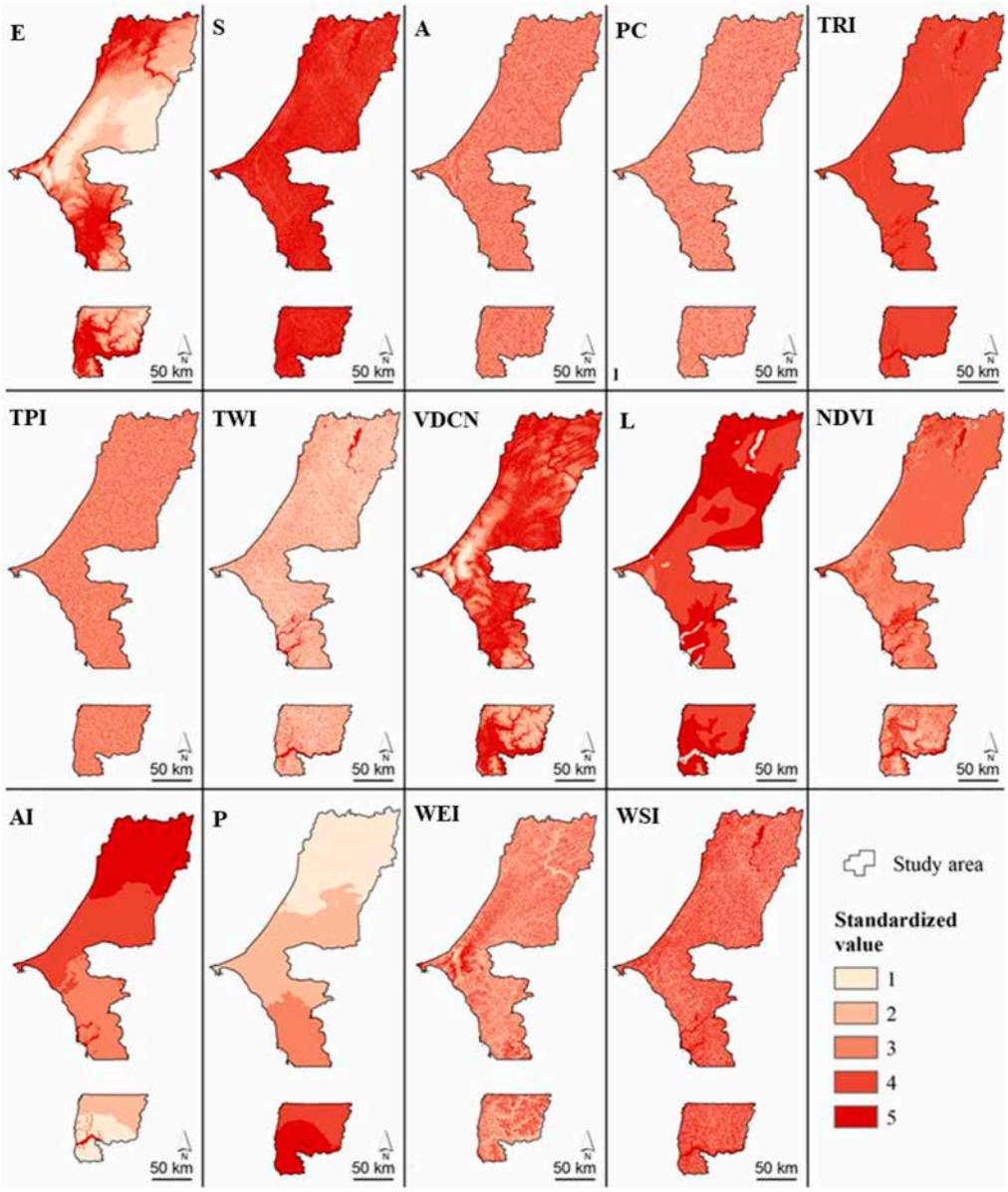

Figure 6. Standardized terrestrial criteria for physical susceptibility to coastal erosion.

The Jenks method has been used in the standardization of the following susceptibility criteria: TWI, TPI, TRI, AI, SWH, NDVI, P, MWS, WSI, and WEI, while the *decision-maker*

standardization method has been used in the standardization of L, S, E, VDCN, PC, A, MFW and B (Table 4). Figure 7 shows standardized marine criteria for physical susceptibility to coastal erosion.

Table 4. Standardized values of criteria for physical susceptibility to coastal erosion.

Standardization Method	Criteria	1 (Very Low)	2 (Low)	3 (Medium)	4 (High)	5 (Very High)
Jenks (natural breaks)	TWI	4.7–8.1	8.2–9.2	9.3–11	12–13	14–25
	TPI	2.2–26	0.64–2.2	−0.68–0.64	−2.3–−0.68	−41–−2.3
	TRI	54–540	20–53	6.4–19	0.01–6.3	0
	AI	5315.87–6744	3649.7–5315.86	2062.88–3649.69	1269.47–2062.87	0–1269.46
	SWH	0–0.55	0.55–0.75	0.75–1	1–1.25	>1.25
	NDVI	0.19–0.49	0.13–0.19	0.09–0.13	0.01–0.09	−0.20–0.01
	P	13–29	29–45	45–66	66–96	96–115
	MWS	2.54–4	4–4.55	4.55–4.9	4.9–5.2	5.2–5.75
	WSI	0.6–5.8	5.8–7.88	7.88–9.83	9.83–11.67	11.67–12.99
	WEI	0.81–0.96	0.96–0.99	0.99–1.03	1.03–1.06	1.06–1.27
Decision-maker	E	>40	20–40	10–20	5–10	0–5
	S	>32	12–32	5–12	2–5	0–2
	VDCN	>40	20–40	10–20	5–10	−5–5
	L	WB *	IVR *	CRS *	SSR *	US *
	PC	Convex	-	Flat	-	Concave
	A	E	NE/SE	Flat/N/S	SW/NW	W
	MFW	0–52,827	52,827–114,827	114,827–169,969	169,969–212,184	212,184–266,131
	B	−30–−81	−10–−30	−5–−10	−2–−5	0–−2

* WB—water bodies, IVR—intermediate volcanic rocks, CSR—carbonate sedimentary rocks, SSR—siliciclastic sedimentary rocks, US—unconsolidated sediment.

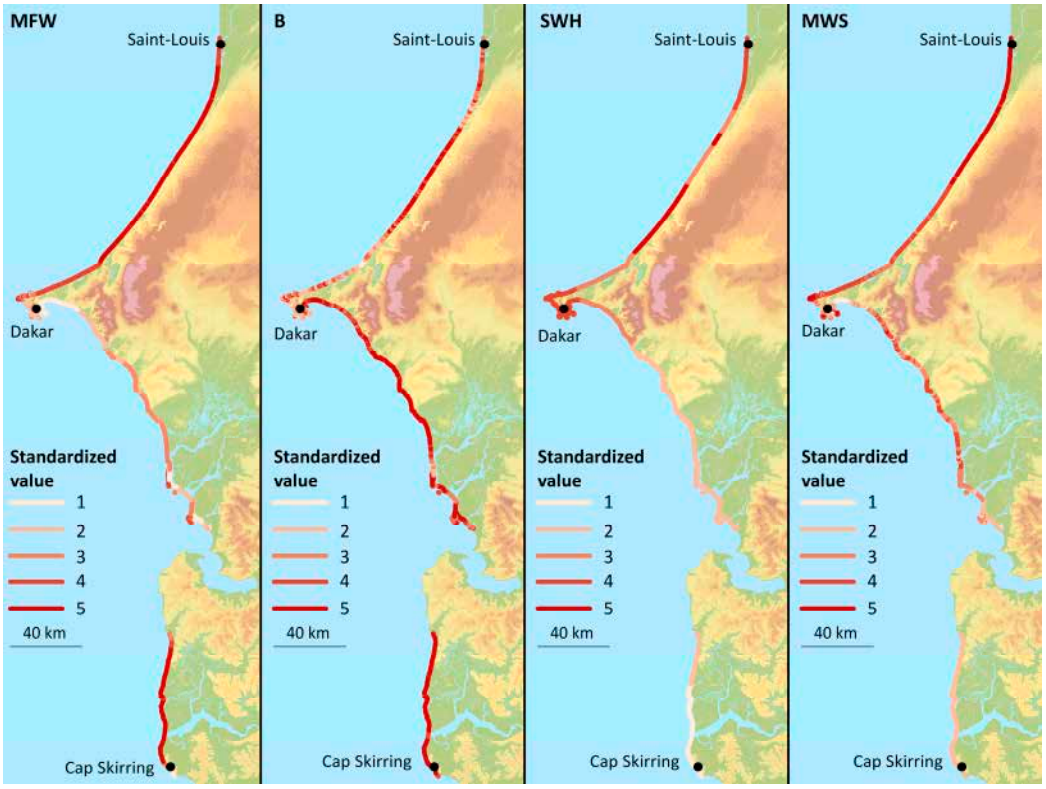

Figure 7. Standardized marine criteria for susceptibility to coastal erosion.

All the socio-economic vulnerability (SVI) criteria apart from the LU/LC have been standardized using the *Jenks* classification method (Table 5). This method is used when experts cannot establish exact class boundaries that would describe susceptibility or vulnerability on a defined scale from 1 to 5. Then, the Jenks method breaks the class values in a way that groups similar values and maximize the differences among classes [96]. The LU/LC has been standardized using the *decision-maker standardization* method. Figure 8 shows the standardized socio-economic criteria for vulnerability to coastal erosion.

Table 5. Standardized values of criteria for socio-economic susceptibility to coastal erosion.

Standardization Method	Criteria	1 (Very Low)	2 (Low)	3 (Medium)	4 (High)	5 (Very High)
Jenks (natural breaks)	PC	0–10.17	10.17–37.3	37.3–122.07	122.07–247.53	247.53–432.34
	PD	0–396.25	396.25–2641.69	2641.69–10,566.76	10,566.76–20,208.94	20,208.94–33,681.56
	RND	0–1.14	1.14–3.42	3.42–8.63	8.63–18.01	18.01–32.34
	HID	0–0.26	0.26–1.36	1.36–3.42	3.42–6.66	6.66–11.17
	EID	0–0.65	0.65–2.66	2.66–5.96	5.96–10.7	10.7–18.31
	DCRIT	0–0.68	0.68–2.55	2.55–5.4	5.4–8.73	8.73–13.25
	DRES	0–83.97	83.97–356.86	356.86–860.67	860.67–1647.87	1647.87–2676.47
Decision-maker	LU/LC	PWB *	M/HW *	TC/SH *	GR/CR *	BUILT/BARE *

* PWB—permanent water bodies, HW—herbaceous wetland, M—mangroves, TC—tree cover, SH—shrubland, GR—grassland, CR—cropland, BUILT—built-up, BARE—bare/sparse vegetation.

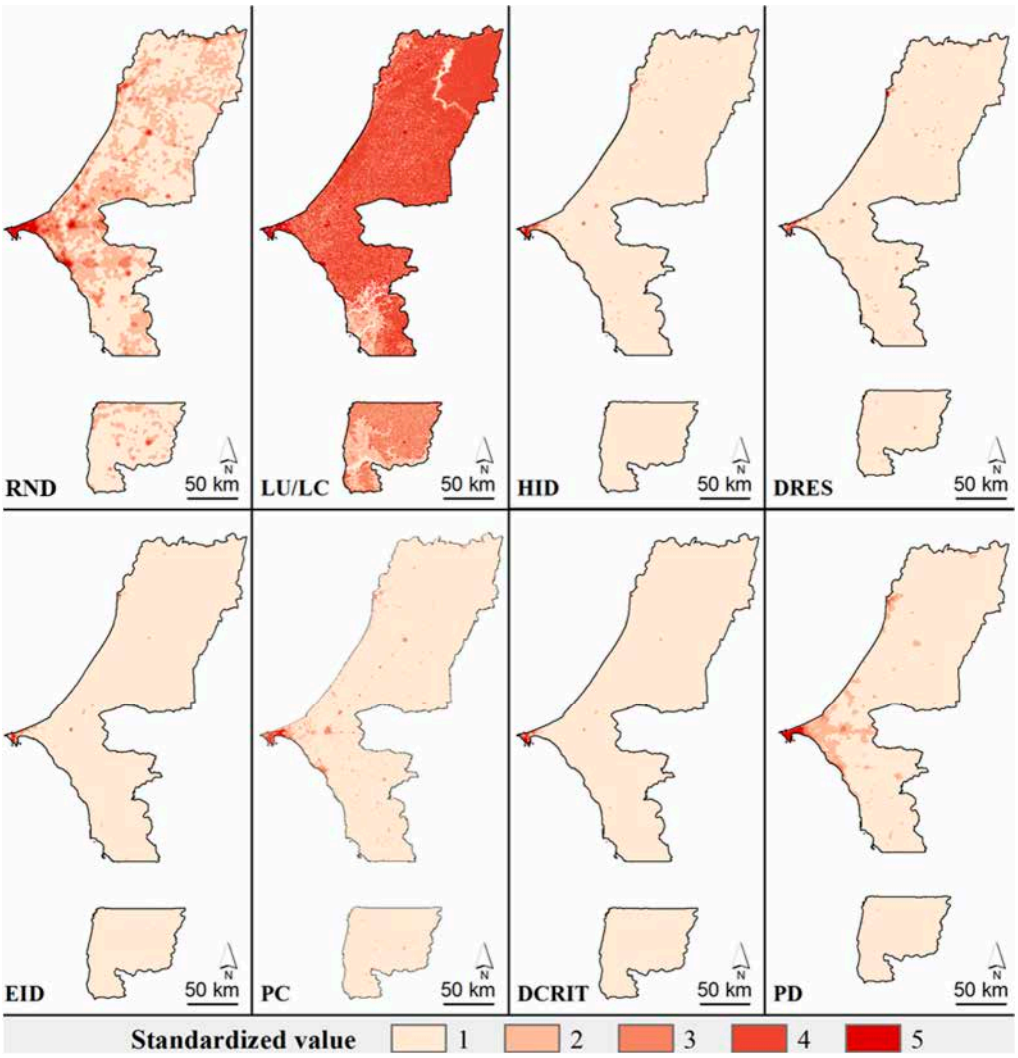

Figure 8. Standardized socio-economic criteria for susceptibility to coastal erosion.

2.4. Weight Coefficients Determination

The weight coefficients (WCs) were determined using the analytical hierarchy process (AHP). Through the derivation of the consistency ratio (CR), the consistency of the weight coefficient calculation was verified. The weight coefficients are consistently determined if the CR value is less than 0.1 [97].

$$CR = \frac{CI}{RI} \quad (1)$$

where:

CI = consistency index

RI = random index

Table 6 shows the WCs determined for the socio-economic vulnerability criteria. (PD) and (PC) are assigned the highest importance due to their role in determining the scale and intensity of social interactions and resource consumption. (LU/LC) follows closely as it can be used as a physical criterion and represents the interaction of society and biophysical material. (DHI) and (DEI) follow since they determine access to essential services, affecting both immediate and long-term resilience against socio-economic shocks. (RDN) has a slightly lower coefficient than (DHI) and (DEI) since the quality of the transport infrastructure is not particularly pronounced for this area. Namely, certain services can be reached even if the roads are blocked, considering that it is a very flat terrain. Lastly, the (DRES) and (DCRIT) are assigned the lowest coefficients, primarily due to the somewhat poorer data quality compared to the other criteria. In addition, (DCRIT) includes, for example, shops and post offices, which, in the context of vulnerability modeling, can be considered less important than hospitals and schools. Overall, this WC determination aligns with the understanding that socio-economic vulnerability is a multifaceted occurrence influenced by various factors, with population dynamics, infrastructure availability, and land use patterns being among the most influential determinants.

Table 6. Weight coefficients of the socio-economic criteria.

	PD	PC	LU/LC	DHI	DEI	RND	DRES	DCRIT	AHP	
PD	1	1	2	3	3	4	4	5	0.249	24.9%
PC	1	1	2	3	3	4	4	5	0.249	24.9%
LU/LC	1/2	1/2	1	2	2	3	4	4	0.157	15.7%
DHI	1/3	1/3	1/2	1	1	2	2	3	0.096	9.6%
DEI	1/3	1/3	1/2	1	1	2	2	3	0.096	9.6%
RND	1/4	1/4	1/3	1/2	1/2	1	1	2	0.058	5.8%
DRES	1/4	1/4	1/3	1/2	1/2	1	1	2	0.058	5.8%
DCRIT	1/5	1/5	1/4	1/3	1/3	1/2	1/2	1	0.037	3.7%
									CR = 0.01888	

Table 7 shows WCs for the terrestrial criteria of physical susceptibility to coastal erosion. (E) has the highest value as it directly influences exposure to coastal processes and inundation risk. (L) follows since it determines the erodibility of coastal landforms. The third is (NDVI), because vegetation cover acts as a natural buffer against erosion. (S) holds importance as it determines the ease of water penetration into the coastal area, although depending on the type of coast, higher slopes can be more susceptible to coastal erosion, mainly through abrasion. (VDCD) and (A) have somewhat higher WCs than the other remaining parameters because they to a greater extent influence the potential hydrological processes and exposure to erosive forces (wind). They are followed by a combination of climatological and morphometric parameters, (P), (WSI), (WEI), and (PC), which are estimated to have less importance. Topographic indices can contribute to coastal erosion susceptibility by capturing landscape morphology, but considering the quality of the input data and the sparse literature, it was decided that they have the lowest weight coefficient.

Table 7. Weight coefficients of the physical (terrestrial) criteria.

	E	L	NDVI	S	VDCN	A	AI	P	WSI	WEI	PC	TPI	TRI	TWI	AHP	
E	1	1	3	4	5	5	6	6	6	6	7	8	8	8	0.224	22.4%
L	1	1	2	3	4	4	5	5	5	5	6	7	7	7	0.187	18.7%
NDVI	1/3	1/2	1	2	3	3	4	4	4	4	5	6	6	6	0.131	13.1%
S	1/4	1/3	1/2	1	2	2	3	3	3	3	4	5	5	5	0.093	9.3%
VDCN	1/5	1/4	1/3	1/2	1	1	2	2	2	2	3	4	4	4	0.063	6.3%
A	1/5	1/4	1/3	1/2	1	1	2	2	2	2	3	4	4	4	0.063	6.3%
AI	1/6	1/5	1/4	1/3	1/2	1/2	1	1	1	1	2	3	3	3	0.040	4.0%
P	1/6	1/5	1/4	1/3	1/2	1/2	1	1	1	1	2	3	3	3	0.040	4.0%
WSI	1/6	1/5	1/4	1/3	1/2	1/2	1	1	1	1	2	3	3	3	0.040	4.0%
WEI	1/6	1/5	1/4	1/3	1/2	1/2	1	1	1	1	2	3	3	3	0.040	4.0%
PC	1/7	1/6	1/5	1/4	1/3	1/3	1/2	1/2	1/2	1/2	1	2	2	2	0.026	2.6%
TPI	1/8	1/7	1/6	1/5	1/4	1/4	1/3	1/3	1/3	1/3	1/2	1	1	1	0.017	1.7%
TRI	1/8	1/7	1/6	1/5	1/4	1/4	1/3	1/3	1/3	1/3	1/2	1	1	1	0.017	1.7%
TWI	1/8	1/7	1/6	1/5	1/4	1/4	1/3	1/3	1/3	1/3	1/2	1	1	1	0.017	1.7%
															CI = 0.0323	

Table 8 shows WCs for the marine criteria of susceptibility to coastal erosion. (SWH) is the most important factor as it represents the primary driver of coastal erosion, with higher wave heights having greater erosive potential. (MFW) follows, as it determines the distance over which waves can build up and generate energy, influencing the intensity of wave action. (MWS) affects wave generation and propagation, influencing the energy transferred to the coastline and subsequently impacting erosion rates. However, it was estimated that it has a smaller influence than the previous two factors. (B), although with a smaller WC, is still important as it defines the underwater topography and can influence wave behavior and erosion patterns. This prioritization aligns with the understanding that coastal erosion is primarily driven by wave dynamics. By assigning higher weights to (SWH) and (MFW), the ranking highlights the significance of wave characteristics in assessing susceptibility to coastal erosion.

Table 8. Weight coefficients of the physical (marine) criteria.

	SWH	MFW	MWS	B	AHP	
SWH	1	2	3	4	0.466	46.6%
MFW	1/2	1	2	3	0.277	27.7%
MWS	1/3	1/2	1	2	0.161	16.1%
B	1/4	1/3	1/2	1	0.096	9.6%
					CI = 0.0146	

2.5. Aggregation of Criteria

The GIS-MCDA aggregation of the selected sub-indices was performed to produce the final integrated coastal erosion vulnerability model (ICER). Derivation was performed using the *Weighted Overlay* tool in ArcMap. First, the terrain and marine criteria of susceptibility to coastal erosion were aggregated in order to produce the physical susceptibility model (PSI). Then, the standardized social-economic criteria have been aggregated in the socio-economic vulnerability index (SVI). Finally, these two models were aggregated into the integrated coastal erosion vulnerability model (ICER). The final ICER model was derived as the sum of the PCI and SVI models with equal weighting coefficients (0.5 and 0.5). In the absence of relevant information on the relative impact of the physical and socio-economic indices, the simple average method (SAM) was chosen. In it, equal weightage to the sub-indices is assigned in order to illustrate the complexity of coastal vulnerability.

2.6. Accuracy Assessment of PSI Model

The validation of the model accuracy has been performed by the overlapping reference data (coastal erosion cadastre sites) with the PSI model using the ROC curve. The ROC curve represents a diagram in which the true positive rate (TPR) values, shown on the y-axis, are placed in relation to the false positive rate (FPR) values, shown on the x-axis of the diagram [47]. For reference data, a coastal erosion cadaster was created based on the analysis of relevant scientific papers, which served as the (TP) sites for the ROC curve creation. A total of 18 (TP) locations were acquired on the coast of Senegal, with attributes of the location, shoreline type, study period, and erosion rate (Table 9). Six (TN) points were manually collected based on locations along sections of Senegal's coast characterized by erosion-resistant lithological units. These TN points serve as references for validating the accuracy of the model's *very low* and *low* susceptibility classes, thus improving the reliability of the created ROC curves. The validation of the PSI model and ROC curve derivation were automated with the ArcSDM tool (extension of ArcMap).

Table 9. Locations of coastal erosion sites (cadastre)—true positive sites.

ID	Sites	Type of Coast	Source	Study Period	Erosion Rate (m)
1	Djiffere	Sandy arrow	[40]	1989–2013	−3.83
2	Saly (Petie Côte)	Sandy beach	[36]	1979–2022	−0.67
3	Popenguine	Sandy/rocky beach	[46]	1954–2022	−0.52
4	Bargny	Sandy beach	[98]	1954–1978	−1
5	Rufisque	Sandy beach	[41]	2006–2022	−0.026
6	Cap-Des-Biches	Rocky beach	[98]	1954–1978	−0.73
7	Mbao	Sandy beach	[98]	1954–1978	−1.4
8	Dakar	Rocky beach	[56]	1954–2015	−1.06
9	Gorée	Sandy beach	[99]	1942–2011	−6.62
10	Guediawaye	Sandy beach	[100]	1942–2011	−0.15
11	Malika	Sandy beach	[100]	1942–2011	−0.15
12	Saint-Louis	Sandy beach	[101]	2004–2020	−2.4
13	presqu'île aux oiseaux	Sandy beach	[21]	1986–2017	−0.98
14	Casamance	Sandy beach	[21]	1968–2017	−6
15	Saint-Louis	Sandy beach	[33]	1984–2016	−3.72
16	Saloum delta	-	[102]	1954–2018	−3.56
17	Palmarin	-	[103]	2014–2018	−3.05
18	Rufisque	Sandy beach	[104]	2008–2018	−6.67

3. Results

3.1. Physical Susceptibility (PSI) and Socio-Economic Vulnerability (SVI) Models

Figure 9 shows the final physical susceptibility (PSI) and socio-economic vulnerability (SVI) to coastal erosion models. The models indicate that areas with high PSI to coastal erosion do not necessarily coincide with areas of high SVI. For example, the coastal zone between Dakar and Saint-Louis has high PSI (Figure 9 between C and B), while the SVI values for that area are low (Figure 9 between G and F). This is because in that area, except for smaller fishing settlements, there is not a large concentration of population and infrastructural density. However, locations with significant socio-economic density (e.g., Dakar and surrounding areas, Saint-Louis and Petite Côte) and landscapes susceptible to coastal erosion can be identified as "hot-spots". These locations are characterized by high PSI and SVI values.

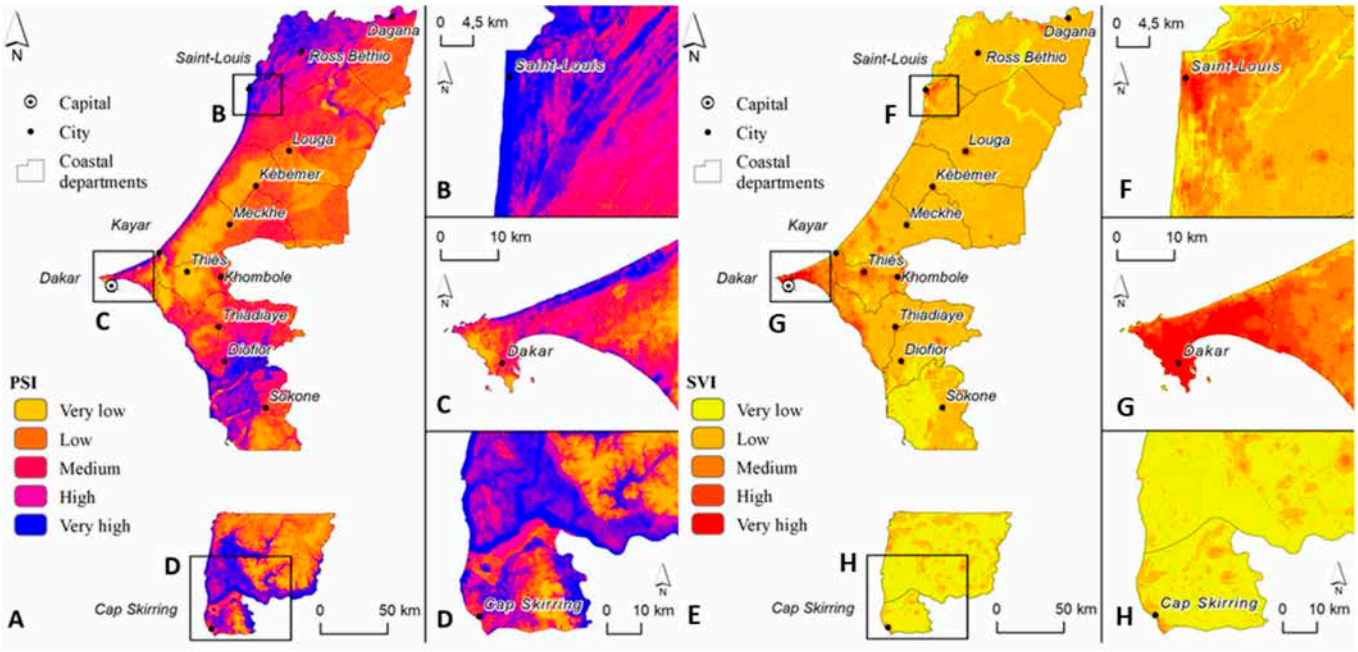

Figure 9. (**A**) Final physical susceptibility (PSI) model to coastal erosion for (**B**) Saint-Louis region, (**C**) Dakar region and (**D**) Cap Skirring region and (**E**) socio-economic vulnerability (SVI) model to coastal erosion for (**F**) Saint-Louis region, (**G**) Dakar region and (**H**) Cap Skirring region.

The PSI reveals a spatial disparity in the coastal erosion susceptibility along the entire Senegal coastal departments, although zones of *high* and *very high* susceptibility dominate near the coastline. In total, the area of classes of *very high* (5) and *high* (4) susceptibility to coastal erosion covers about 28% of the total area of coastal departments (Table 10). It is easy to see that the unconsolidated sediments, mainly sandy coasts, are marked by significant erosion, namely Saint-Louis (north coast of Senegal) (B), Cap-Skiring (D), and the sandy spits of the Saloum islands (C) to the south of Dakar (Figure 9).

The Saint-Louis area is the first recognized as a "hot spot" of susceptibility to coastal erosion. It is susceptible to coastal erosion due to the delta formation: low-lying areas naturally prone to erosion from both tidal action and wave energy, especially during storms and high tides. The coastline around Saint-Louis experiences significant wave action and currents from the Atlantic Ocean. The coast around Dakar, including beaches such as Yoff and Ngor, is exposed to strong waves and human activities that can exacerbate erosion. The secure storage areas for fishing boats are decreasing in this area, and fishing docks are being destroyed. The main fishing points (Yoff, Soumbedioune, Hann, etc.) are particularly vulnerable to the impacts of coastal erosion. The Cape Verde peninsula to the west of Dakar, on the other hand, is not much affected by coastal erosion (C). This may be due to the nature of the coastline, which is essentially made from erosion-resistant volcanic rocks. The coast of Petite Côte, with the exception of certain hot spots on the coast, in relation to the entire coastal area of Senegal, is located in the medium PSI class. This area is known for its tourist settlements and sandy beaches. However, intensive tourism development and changes in land use may contribute to greater susceptibility to erosion. For example, the location with very high PSI in this area is the seaside resort of Saly Portudal, 80 km from Dakar. Its predominantly sandy coastline comprises narrow beaches (10 to 70 m) and low-profile topography. The Saloum Delta in the PSI model is dominantly recognized as an area of *very high* physical susceptibility. The Saloum Delta is rich in biodiversity, inhabited by more than 100,000 people. Although this tropical mangrove ecosystem can mitigate the erosive impact of waves, its ecosystem is currently under pressure because of climate change and unsustainable use of the mangrove forests. The next area that is dominantly classified as a high PSI area is the northern Lower Casamance. It is an area known for its

river estuaries and mangrove forests, which is subject to a wide range of hazards mainly caused by climate change. The detected coastal erosion susceptibility is consistent with the results of previous research on coastal erosion along the Senegalese coast (Table 9).

Table 10. Area and percentage of PSI and SVI classes for departments.

PSI Classes	Area (km^2)	Percentage (%)	SVI Classes	Area (km^2)	Percentage (%)
1 (very low)	6135.3	17.53	1 (very low)	10,537.84	30.12
2 (low)	10,710.8	30.61	2 (low)	21,668.57	61.92
3 (medium)	8183.7	23.39	3 (medium)	2288.92	6.54
4 (high)	5454.0	15.59	4 (high)	388.56	1.11
5 (very high)	4507.9	12.88	5 (very high)	107.78	0.31

The SVI model shows that Dakar and Saint-Louis are the locations most socio-economically vulnerable to coastal erosion (Figure 9). This situation is the result of a strong presence of coastal infrastructure (people and their property). These areas are characterized by strong urban growth, which translates into high levels of anthropization. On the other hand, sites such as Cap-Skiring and the Saloum islands (south of Dakar), which are not vulnerable, are not socially or economically exposed. Given that the population in Senegal's coastal areas is concentrated in a few larger cities, the area of *very high* (5) and *high* (4) socio-economic vulnerability to coastal erosion is small and includes only 1.3% of the total area of the coastal departments.

3.2. Final Integrated Coastal Erosion Vulnerability Model (ICER)

Figure 10 shows the final integrated coastal erosion vulnerability model (ICER) derived on the basis of the PSI and SVI. Both the PSI and SVI had the same weight coefficient (0.5) in the derivation of the ICER.

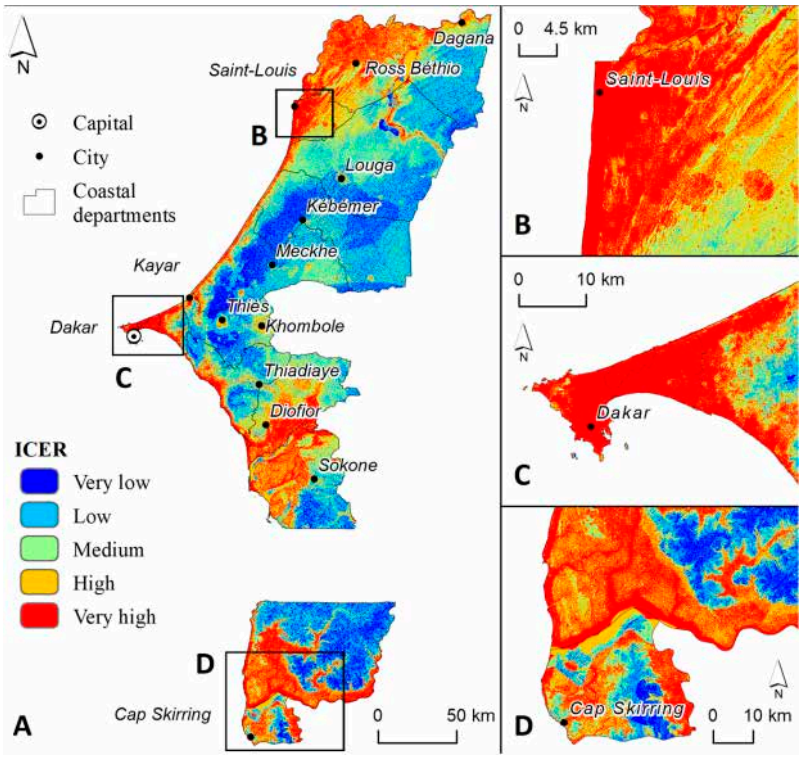

Figure 10. (**A**) Integrated coastal erosion vulnerability model (ICER) for (**B**) Saint-Louis region, (**C**) Dakar region and (**D**) Cap Skirring region.

The very high (5) and *high* (4) classes within the ICER cover around 31% of the coastal departments' total area (Table 11), mostly encompassing a narrow coastal strip and low river valleys and mouths characterized by a high degree of anthropization and coastline development, as well as geological and geomorphological features that increase their susceptibility to coastal erosion. These models have shown that sections of the Senegalese coastline, namely Dakar, Saint-Louis and Casamance, are major hotspots, i.e., areas that are highly vulnerable to coastal erosion.

Table 11. Area and percentage of ICER classes for coastal departments.

ICER Classes	Area (km^2)	Percentage (%)
1 (very low)	5218.5	14.91
2 (low)	10,454.6	29.88
3 (medium)	8145.7	23.28
4 (high)	5607.8	16.03
5 (very high)	5565.1	15.90

4. Discussion

4.1. Coastal Erosion in Senegal

In this paper, we have assessed the susceptibility and vulnerability of Senegal's coastal zone to coastal erosion using a GIS-MCDA approach. This method, on this scale and with this number of criteria, was being used for the first time for the coast of Senegal with the aim of quantifying or identifying sectors vulnerable to coastal erosion. Data from various, mostly open, sources was used. The PSI and SVI were used to generate the ICER, while additionally, a spatial analysis was carried out to identify sections of the Senegalese coastline vulnerable to coastal erosion. The indices obtained were used to map vulnerability to coastal erosion and to classify these areas according to their level of vulnerability. This vulnerability does not appear to be uniform along the Senegalese coastline. The entire Senegalese coastline can be regarded as somewhat vulnerable to coastal erosion, but it is important to point out that this vulnerability does not appear to be uniform along the coastline, indicating a degree of spatial variability, where Saint-Louis and parts of Dakar are the most exposed to coastal erosion.

In Dakar, it is easy to see that virtually the entire coastline of the region is eroding (Figure 10). The only exception is a small portion of the region, located more precisely on the Cape Verde peninsula, that is at low risk. This reflects the geological, geomorphological and bioclimatic conditions of the Cape Verde peninsula, which is also characterized by the presence of cliffs with hard lithological features. According to [105], the rocky coasts are retreating less rapidly than the sandy coasts. Furthermore, the work of [100] highlights erosion rates estimated at -0.15 m/year on the Cape Verde peninsula between 1942 and 2011. However, apart from the Cape Verde peninsula, much of the Dakar region is characterized by the presence of sandy beaches, which explains the erosive dynamics of its beaches. This erosion has a considerable impact on the socio-economic activities developed in Dakar. Assessing the potential economic losses likely to be caused by coastal erosion in Dakar in 2030 and 2040, the paper of [106] reports economic losses estimated at 38,507,856,000 and 57,822,698,000 CFA francs, respectively. Furthermore, like the capital Dakar, the Petite Côte, located to the south of Dakar, is vulnerable to coastal erosion. As a highly urbanized area, the Petite Côte suffers the full force of erosion, which results in the destruction of human habitats and the decline of socio-economic activities such as trade, tourism, fishing and related activities. Numerous studies carried out in the area indicate that coastal erosion is an obstacle to socio-economic activities [62,107–110].

In addition, as the coast is essentially made up of unconsolidated sandy beaches, the susceptibility to coastal erosion increases as you head north, particularly on the Grande Côte (from Yoff to Saint-Louis). However, it seems clear that the northern section of

the coast is the most sensitive to coastal erosion. It should be noted that the factors explaining this erosion have already been mentioned. These regions are characterized by a high degree of anthropization and coastline development, as well as geological and geomorphological features that increase their vulnerability to coastal erosion [37,111–113], but also by its high-energy wave climates [34]. For example, the Saint-Louis coastline, particularly the Langue de Barbarie, is located on a low sandy barrier beach that is highly sensitive to coastal erosion [114,115]. According to [116], due to its distinctive physical and socio-economic characteristics, the Saint-Louis region is among the areas in Senegal most vulnerable to the adverse impacts of coastal erosion. Today, most morphodynamic studies carried out in Senegal identify the Saint-Louis coastline as being the most vulnerable to coastal erosion [117]. In this area, erosion persists as a significant social, economic, and environmental issue. In addition to causing economic and environmental damage, it has also resulted in the disappearance of certain villages, such as Doun Baba Dièye [118]. Our results are fully consistent with those of [33,36,101,116,119].

In the Lower Casamance, erosion is variable, with the Cap-Skiring sector showing low erosion rates. To the north of this area, toward Kafaountine, Carabane and Diogué, erosion is very intense. Research carried out on the Lower Casamance coast by [120–123] shows that this part of the coast is vulnerable to coastal erosion. The erosive dynamics observed on the Casamance coast are likely to increase, especially in the context of the exploitation of resources. Indeed, ref. [124] argues that zircon mining is a catalyst for the coastal erosion observed along the Lower Casamance coastline. As with other sites, coastal erosion is a real obstacle to the area's influence and economic development. The research of [123,125–127] has clearly shown that the retreat of the coastline is changing the geographical landscape of the region, causing the silting up of mangroves and the salinization of the land, with the consequent loss of rice fields.

Several studies show that natural factors have a determining influence on the evolution of coastlines [103,128], but some results indicate that human activities can be the main cause of coastal erosion [129]. In fact, the areas most exposed to erosion on the Senegalese coast are those characterized by a strong human presence. This is mainly due to the greater population and employment density in these regions, namely Dakar, Saint-Louis and Mbour (Petite Côte). Coastal areas are socially and economically very important, which leads to strong human convergence [130]. Hence, the staggering financial cost of the degradation of Senegal's coastal zones, estimated at USD 537 million, which corresponds to a slowdown in GDP of around 3.3% [131].

As the ROC curves indicate the high accuracy of the created GIS-MCDA model, it can be considered as a valuable tool for coastal management and planning initiatives. Its performance metrics indicate strong discriminatory power and suggest that the derived models can be a valuable tool for coastal management and planning initiatives. Our results are in line with those of [21,35,37,40,41,43,56,116,127]. These studies have shown that sections of the Senegalese coastline, namely Dakar, Saint-Louis and Casamance, are major hotspots, i.e., areas that are highly vulnerable to coastal erosion.

The ICER has a few advantages over existing coastal vulnerability indices. The ICER integrates 26 criteria (18 for physical susceptibility and eight for social-economic vulnerability). This approach provides a more detailed assessment compared to simpler indices of coastal vulnerability, which typically use fewer criteria. By deriving two sub-indices (PSI and SVI) specific to Senegal's coastal departments, the ICER accounts for local variations in susceptibility to coastal erosion and social-economic vulnerability. This customization ensures that the model is more relevant and accurate for the region compared to generalized indices.

Even though the resulting model faithfully reflects the realities, it is important to point out that the diversity of the data sources used in the work and the disparate spatial and temporal resolutions may affect the results. Furthermore, in the context of climate change, the sea-level rise is a real threat to coastal areas [132–135]. Moreover, a host of studies have shown that the sea-level rise makes coasts more vulnerable to coastal erosion [136–143].

However, in the context of this research, it is clear that the parameter of the sea-level rise is not included in the model input data, which risks minimizing the vulnerability of the coastal erosion risk on the line under study. Thus, in the future, for a good understanding of the risk of marine submersion, it is important to take these parameters into account for a complete modeling of the coastal erosion phenomenon.

4.2. Accuracy Assessment of PSI

The AUC value represents the measure of accuracy of an analyzed model in relation to the reference data, where excellent (0.9–1), very good (0.8–0.9), good (0.7–0.8), bad (0.6–0.7) and unsuccessful (0.5–0.6) models can be differentiated [47]. If just the TP sites are considered, the AUC value for the PSI model is 0.881, which proves that the created model achieves very good accuracy in the determination of coastal erosion susceptibility (Figure 11B). However, if both the TP and TN sites are considered, the AUC values are even higher. An AUC of 0.907 indicates that the PSI model performs very well in distinguishing locations where coastal erosion is observed (TP sites) from those where it is not (TN sites) (Figure 11C). This suggests that the PSI model has high capability in identifying areas prone to erosion based on the considered physical, marine, and terrestrial susceptibility criteria. It also accurately identifies locations where coastal erosion is not occurring.

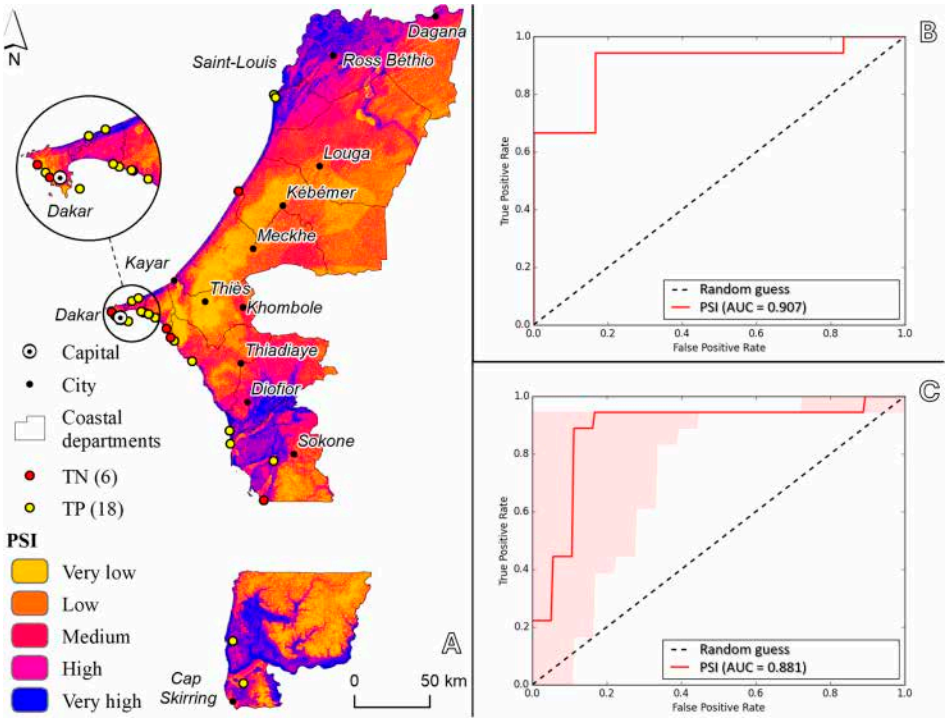

Figure 11. PSI accuracy assessment using the ROC curves (**A**), using the TP sites (**B**) and using both the TP and TN sites (**C**).

5. Conclusions

This research derived the ICER model by the aggregation of the PSI and SVI models using the GIS-MCDA approach. The PSI model shows a spatial disparity regarding susceptibility to erosion within coastal departments with a share of *very high* (5) and *high* (4) classes of about 28%. Unconsolidated, mainly sandy coasts are recognized as the areas most susceptible to erosion, namely Saint-Louis (north coast of Senegal), Cap-Skiring, and the sandy spits of the Saloum islands (C) to the south of Dakar. The Cape Verde peninsula to the west of Dakar, on the other hand, is not much affected by coastal erosion. In the SVI model, densely populated areas and built-up areas are recognized as most vulnerable to coastal erosion, where Dakar and St. Louis stand out. Given that the population in Senegal's coastal areas is concentrated in few larger cities, the area of *very high* (5) and *high*

(4) socio-economic vulnerability to coastal erosion is small and includes only 1.3% of the total area of the coastal departments.

Both the PSI and SVI models had the same weight coefficient (0.5) in the derivation of the ICER. *The very high* (5) and *high* (4) ICER areas cover around 31% of the coastal departments' total area, mostly encompassing a narrow coastal strip and low river valleys and mouths characterized by a high degree of anthropization and coastline development, as well as geological and geomorphological features that increase their susceptibility to coastal erosion. These models have shown that sections of the Senegalese coastline, namely Dakar, Saint-Louis and Casamance, are major hotspots, i.e., areas that are highly vulnerable to coastal erosion. The AUC for the TP and TN sites generated values of 0.907 and 0.881 values for the PSI model, making it reliable for predicting coastal erosion sites.

The derived sub-indices are important in order to determine coastal vulnerability based on a socio-ecological approach. This research relies on the integration of natural (terrestrial and marine) and socio-economic criteria to determine their mutual interaction in describing the vulnerability to coastal erosion. The utility of the ICER is the ability to provide a detailed, in the context of the regional scale of research (coastal departments of Senegal), and accurate assessment of integrated coastal vulnerability, which is essential for informed decision-making. The efficiency of the ICER lies in the use of open-source data and the GIS-MCDA method, which enables the integration of complex datasets. This approach can help with the detection and prioritization of areas in which intervention in the context of mitigation of coastal erosion problems is necessary.

This study and the derived models can serve as a decision support tool for the construction of an appropriate integrated coastal zone management (ICZM) model for Senegal's coastal zone.

Author Contributions: Conceptualization, C.O.T.C. and I.M.; methodology, F.D. and C.O.T.C.; software, I.M. and F.D.; validation, F.D., K.G. and C.O.T.C.; formal analysis, C.O.T.C. and I.M.; data curation, F.D.; writing—original draft preparation, C.O.T.C. and I.M.; writing—review and editing, C.O.T.C., I.M., K.G. and R.A.; visualization, F.D.; supervision R.A., C.O.T.C. and I.M. All authors have read and agreed to the published version of the manuscript.

Funding: This research received no external funding.

Institutional Review Board Statement: Not applicable.

Informed Consent Statement: Not applicable.

Data Availability Statement: The dataset is available on request from the authors.

Conflicts of Interest: The authors declare no conflicts of interest.

References

1. Nourdi, N.F.; Raphael, O.; Grégoire, A.O.; Paul, R.J.; Sakaros, B.; Thomas, S.; Minette, T.E. Seasonal to decadal scale shoreline changes along the Cameroonian coastline, Bay of Bonny (1986 to 2020). *Reg. Stud. Mar. Sci.* **2021**, *45*, 101798. [CrossRef]
2. Luijendijk, A.; Hagenaars, G.; Ranasinghe, R.; Baart, F.; Donchyts, G.; Aarninkhof, S. The state of the world's beaches. *Sci. Rep.* **2018**, *8*, 6641. [CrossRef] [PubMed]
3. Castillo, V.R.; Negro Valdecantos, V.; del Campo, J.M. Understanding the impact of hydrodynamics on coastal erosion in Latin America: A systematic review. *Front. Environ. Sci.* **2023**, *11*, 1267402. [CrossRef]
4. Molua, O.C.; Ukpene, A.O.; Vwavware, J.O.; Nwachuku, D.N.; Osuhor, P.O. Geophysical Assessment of Coastal Erosion in Nigeria's Coastal Regions: Strategies for Protection and Management. *Int. J. Res. Sci. Eng.* **2021**, *1*, 2394–8299. [CrossRef]
5. Toimil, A.; Camus, P.; Losada, I.J.; Le Cozannet, G.; Nicholls, R.J.; Idier, D.; Maspataud, A. Climate change-driven coastal erosion modelling in temperate sandy beaches: Methods and uncertainty treatment. *Earth-Sci. Rev.* **2020**, *202*, 103110. [CrossRef]
6. Pang, T.; Wang, X.; Nawaz, R.A.; Keefe, G.; Adekanmbi, T. Coastal erosion and climate change: A review on coastal-change process and modeling. *Ambio* **2023**, *52*, 2034–2052. [CrossRef]
7. Sinay, L.; Carter, R.W. Climate change adaptation options for coastal communities and local governments. *Climate* **2020**, *8*, 7. [CrossRef]
8. Harvey, N.; Nicholls, R. Global sea-level rise and coastal vulnerability. *Sustain. Sci.* **2008**, *3*, 5–7. [CrossRef]
9. Jie, S.; Wenhuan, Z.; Yantao, Y.; Shoujin, L.; Yingci, F. Current situation and influence factors of coastal erosion in Guangdong. *Acta Oceanol. Sin.* **2015**, *37*, 142–152.

10. Paskoff, R. Conséquences possibles sur les milieux littoraux de l'élévation du niveau de la mer prévue pour les prochaines décennies. In *Annales de Géographie*; Armand Colin: Paris, France, 1998; Volume 107, pp. 233–248. [CrossRef]
11. Salman, A.; Lombardo, S.; Doody, P. *Living with Coastal Erosion in Europe: Sediment and Space for Sustainability*; Eurosion Project Reports; TU Delft Research Repository: Delft, The Netherlands, 2004.
12. Faye, I. Dynamique du Trait de Côte sur les Littoraux Sableux de la Mauritanie à la Guinée-Bissau, (Afrique de l'Ouest): Approches Régionale et Locale par Photo Interprétation Traitement D'images et Analyse de Cartes Anciennes. Ph.D. Thesis, Université de Bretagne Occidentale, Brest, France, 2010; 401p.
13. Wang, J.; Gao, W.; Xu, S.; Yu, L. Evaluation of the combined risk of sea level rise, land subsidence, and storm surges on the coastal areas of Shanghai, China. *Clim. Chang.* **2012**, *115*, 537–558. [CrossRef]
14. Vousdoukas, M.I.; Voukouvalas, E.; Mentaschi, L.; Dottori, F.; Giardino, A.; Bouziotas, D.; Bianchi, A.; Salamon Feyen, L. Developments in large-scale coastal flood hazard mapping. *Nat. Hazards Earth Syst. Sci.* **2016**, *16*, 1841–1853. [CrossRef]
15. Goussard, J.J.; Ducrocq, M. West African coastal area: Challenges and outlook. In *The Land/Ocean Interactions in the Coastal Zone of West and Central Africa*; Springer: Berlin/Heidelberg, Germany, 2014; pp. 9–21. [CrossRef]
16. Pradhan, U.; Mishra, P.; Mohanty, P.K.; Behera, B. Formation, growth and variability of sand spit at Rushikulya river mouth, south Odisha coast, India. *Procedia Eng.* **2015**, *116*, 963–970. [CrossRef]
17. Alves, B.; Angnuureng, D.B.; Morand, P.; Almar, R. A review on coastal erosion and flooding risks and best management practices in West Africa: What has been done and should be done. *J. Coast. Conserv.* **2020**, *24*, 38. [CrossRef]
18. Heger, M.; Vashold, L.; Palacios, A.; Alahmadi, M.; Acerbi, M. *Blue Skies, Blue Seas: Air Pollution, Marine Plastics, and Coastal Erosion in the Middle East and North Africa*; World Bank Publications: Chicago, IL, USA, 2022. [CrossRef]
19. Charuka, B.; Angnuureng, D.B.; Brempong, E.K.; Agblorti, S.K.; Agyakwa KT, A. Assessment of the integrated coastal vulnerability index of Ghana toward future coastal infrastructure investment plans. *Ocean Coast. Manag.* **2023**, *244*, 106804. [CrossRef]
20. Allersma, E.; Tilmans, W.M. Coastal conditions in West Africa—A review. *Ocean Coast. Manag.* **1993**, *19*, 199–240. [CrossRef]
21. Thior, M.; Sane, T.; Sy, O.; Descroix, L.; Ba, B.D.; Solly, B.; Mendy, V. Spatial analysis of the evolution of the coastline around the mouth of the Casamance River (Senegal) from 1968 to 2017, using the DSAS tool. *Eur. Sci. J.* **2019**, *15*, 1857–7881. [CrossRef]
22. Tchindjang, M.; Mbevo, F.P.; Bopda, A. Chapitre 22. Une Afrique Atlantique avec des villes sous l'eau ! Construire des villes côtières sans inondations? In *Construire La Ville Portuaire De Demain En Afrique Atlantique*; Editions EMS: Caen, France, 2019; 30p.
23. Nhantumbo, J.B.; Dada, O.A.; Ghomsi, F.E.K. *Sea Level Rise and Climate Change—Impacts on African Coastal Systems and Cities*; IntechOpen: London, UK, 2023. [CrossRef]
24. Anthony, E.; Almar, R.; Besset, M.; Reyns, J.; Laibi, R.; Ranasinghe, R.; Ondoa, G.A.; Vacchi, M. Response of the Bight of Benin (Gulf of Guinea, West Africa) coastline to anthropogenic and natural forcing, Part 2: Sources and patterns of sediment supply, sediment cells, and recent shoreline change. *Cont. Shelf Res.* **2019**, *173*, 93–103. [CrossRef]
25. Mbevo Fendoung, P.; Tchindjang, M.; Hubert-Ferrari, A. Weakening of Coastlines and Coastal Erosion in the Gulf of Guinea: The Case of the Kribi Coast in Cameroon. *Land* **2022**, *11*, 1557. [CrossRef]
26. Dada, O.A.; Almar, R.; Morand, P. Coastal vulnerability assessment of the West African coast to flooding and erosion. *Sci. Rep.* **2024**, *14*, 890. [CrossRef]
27. Goussard, J.J. Presentation of the West African Coastal Risk Prevention Plan and the West African Coastal Observation Mission. In Proceedings of the International Conference on Knowledge and Understanding of Coastal Risks: Hazards, Issues, Representations, Management, Brest, France, 3–4 July 2014; pp. 154–162.
28. Angnuureng, B.D.; Adade, R.; Chuku, E.O.; Dzantor, S.; Brempong, E.K.; Mattah PA, D. Effects of coastal protection structures in controlling erosion and livelihoods. *Heliyon* **2023**, *9*, e20633. [CrossRef]
29. Lacroix, D.; Mora, O.; Menthière, N.; et Béthinge, A. Sea level rise: Consequences and anticipations by 2100, the light of foresight. *Study Rep. Natl. Environ. Res. Alliance* **2019**, *51*, 172.
30. Stocker, T.F.; Qin, D.; Plattner, G.-K.; Tignor, M.; Allen, S.K.; Boschung, J.; Nauels, A.; Xia, Y.; Bex, V.; Midgley, P.M. (Eds.) IPCC Summary for Policymakers. In *Climate Change 2013: The Physical Science Basis. Contribution of Working Group I to the Fifth Assessment Report of the Intergovernmental Panel on Climate Change*; Cambridge University Press: Cambridge, UK; New York, NY, USA, 2013.
31. Sergent, P.; Prevot G et Trmal, C. Reinforcing shallow structures against rising sea levels. In Proceedings of the "Impacts of Climate Change on Coastal Risks" Conference, Orleans, France, 15–16 November 2010; pp. 147–151.
32. Dabo, M.; Gning, I.; Mamadou et Diallo, A.D. Coastal erosion, climate change and tectonics: Impacts on the Senegalese coast between Dakar and Mbour (Western Senegal). *J. Confluens* **2015**, *1*, 10–11.
33. Ndour, A.; Laïbi, R.A.; Sadio, M.; Degbe, C.G.; Diaw, A.T.; Oyédé, L.M.; Anthony, E.J.; Dussouillez, P.; Sambou, H.; Dièye, E.H.B. Management strategies for coastal erosion problems in west Africa: Analysis, issues, and constraints drawn from the examples of Senegal and Benin. *Ocean Coast. Manag.* **2018**, *156*, 92–106. [CrossRef]
34. Cisse, C.O.T.; Brempong, E.K.; Taveneau, A.; Almar, R.; Sy, B.A.; Angnuureng, D.B. Extreme coastal water levels with potential flooding risk at the low-lying Saint Louis historic city, Senegal (West Africa). *Front. Mar. Sci.* **2022**, *9*, 993644. [CrossRef]
35. Cissé CO, T.; Taveneau, A.; Almar, R.; Bergsma EW, J. Satellite monitoring of the evolution of developed beaches: The example of the Petite Côte (Senegal, West Africa). *Photo Interpret. Eur. J. Appl. Remote Sens.* **2022**, *58*, 45–56. [CrossRef]
36. Yade, D. Coastal Erosion and Adaptation Strategies in the Face of Climate Variability on Senegal's Petite-Côte: The Case of the Communes of Mbour and Saly Portudal (Senegal). Master's Thesis, UFR Des Sciences et Technologies Department of Geography, Assane Seck University, Ziguinchor, Senegal, 2022; 132p.

37. Niang-Diop, I. Coastal Erosion on the Small Senegalese Coast, Using the Example of Rufisque the Example of Rufisque. Ph.D. Thesis, University of Anger, Angers, France, 1996; 285p.
38. Brüning, L. Coastal Erosion in Northern Senegal: Migration and Adaptation Strategies. Ph.D. Thesis, Institute of Geography, University of Neuchâtel, Neuchâtel, Switzerland, 2022; 262p. [CrossRef]
39. Diombera, M. Aménagement et Gestion Touristiques Durables du Littoral Sénégalais de la Petite Côte et de la Basse Casamance. Ph.D. Thesis, Université Gaston Berger de Saint-Louis, Saint-Louis, Senegal, 2011; 343p.
40. Diadhiou, Y.; Ndour, A.; Niang, I.; Fall-Niang, A. Comparative study of shoreline evolution on two sandy spits of the little coast (Senegal): The cases of Joal and Djiffère. *Norois* **2016**, *240*, 25–42. [CrossRef]
41. Cissé, C.O.T.; Youm, J.P.M.; Sy, B.A.; Almar, R.; Kader, B.A. Évolution du trait de côte dans la zone urbanisée de Rufisque et de Mbao (Sud-ouest du Sénégal) sur la séquence temporelle 2006–2022: Entre exploitation et protection du littoral. *Espace Géographique et Société Marocaine* **2023**, *1*, 71.
42. Bongarts Lebbe, T.; Rey-Valette, H.; Chaumillon, É; Camus, G.; Almar, R.; Cazenave, A.; Claudet, J.; Rocle, N.; Meur-Ferec, C.; Viard, F.; et al. Designing coastal adaptation strategies to tackle sea level rise. *Front. Mar. Sci.* **2021**, *8*, 740602. [CrossRef]
43. Ndour, A. Evolution Morpho-Sédimentaire et Impacts des Ouvrages de Protection sur le Littoral de Dakar, Petite Côte. Ph.D. Thesis, Cheikh Anta Diop University in Dakar, Dakar, Senegal, 2015; 243p.
44. Marone, A. Diagnosis of Continental and Marine Flood Risks: Application to the Communes of Rufisque (Senegal). Ph.D. Thesis, University of Caen, Caen, France, 2016; p. 427.
45. Ngom, H.; Ndour, A.; Niang, I. Impacts of protective structures on sandy beaches: Example of the Saly balnear station, Petite Côte, Senegal. *J. Coast. Res.* **2018**, *81*, 114–121. [CrossRef]
46. Youm, J.P.; Cisse CO, T.; Ba Ket Sagne, P. Kinematics of the coastline of a coastline with high cult values from 1952 to 2022: The case of Popenguine (Little Coast, Senegal). *Belgeo*, 2024, *in press*.
47. Domazetović, F.; Šiljeg, A.; Lončar, N.; Marić, I. Development of automated multicriteria GIS analysis of gully erosion susceptibility. *Appl. Geogr.* **2019**, *112*, 102083. [CrossRef]
48. Šiljeg, A.; Šiljeg, S.; Milošević, R.; Marić, I.; Domazetović, F.; Panđa, L. Multi-hazard susceptibility model based on high spatial resolution data—A case study of Sali settlement (Dugi otok, Croatia). *Environ. Sci. Pollut. Res.* **2024**, *31*, 40732–40747. [CrossRef] [PubMed]
49. Cutter, S.L.; Emrich, C.T.; Webb, J.J.; Morath, D. Social vulnerability to climate variability hazards: A review of the literature. *Final Rep. Oxfam Am.* **2009**, *5*, 1–44.
50. Dewan, A. Floods in a megacity: Geospatial techniques in assessing hazards. In *Chapter 2: Hazards, Risk, and Vulnerability*; Springer Geography: Dordrecht, The Netherlands, 2013. [CrossRef]
51. Alcántara-Carrió, J.; García Echavarría, L.M.; Jaramillo-Vélez, A. Is the coastal vulnerability index a suitable index? Review and proposal of alternative indices for coastal vulnerability to sea level rise. *Geo-Mar. Lett.* **2024**, *44*, 8. [CrossRef]
52. Gornitz, V. Global coastal hazards from future sea level rise. *Palaeogeogr. Palaeoclimatol. Palaeoecol.* **1991**, *89*, 379–398. [CrossRef]
53. Roukounis, C.N.; Tsihrintzis, V.A. Indices of coastal vulnerability to climate change: A review. *Environ. Process.* **2022**, *9*, 29. [CrossRef]
54. Yahia Meddah, R.; Ghodbani, T.; Senouci, R.; Rabehi, W.; Duarte, L.; Teodoro, A.C. Estimation of the Coastal Vulnerability Index Using Multi-Criteria Decision Making: The Coastal Social–Ecological System of Rachgoun, Western Algeria. *Sustainability* **2023**, *15*, 12838. [CrossRef]
55. Wang, X.; Zhang, W.; Yin, J.; Wang, J.; Ge, J.; Wu, J.; Luo, W.; Lam, N.S. Assessment of coastal erosion vulnerability and socio-economic impact along the Yangtze River Delta. *Ocean Coast. Manag.* **2021**, *215*, 105953. [CrossRef]
56. Bakhoum, P.W.; Niang, I.; Sambou, B.; et Diaw, A.T. Une presqu'île en érosion cotiere ? Dakar, la capitale sénégalaise face à la montée de la mer dans le contexte de changement climatique. *Environ. Water Sci.* **2018**, *2*, 91–108.
57. CSE Centre de Suivi Ecologie. *Annuaire Sur L'environnement et Les Ressources Naturalles du Sénégal*; Ministere de l'Environnement et du Developpement Durable; CSE Centre de Suivi Ecologie: Dakar, Senegal, 2013; 338p.
58. Sow, A. Evolution Morphosedimentary the Beaches of the Petite Côte: Case of the Seaside Resort of Saly (Senegal). Master's Thesis, Assane Seck University of Ziguinchor, Ziguinchor, Senegal, 2018; 115p.
59. Turmine, V. La Dynamique Littorale Entre Mbour et Joal (Petite Côte -Sénégal) Conséquences. Master's Thesis, Université de Paris VII Denis Diderot, Paris, France, 2000; 255p.
60. Sall, M. Dynamique et Morphogénèse Actuelles au Sénégal Occidental. Université Louis Pasteur: Strasbourg, France, 1982; 682p.
61. Gningue, I. Contribution à L'étude Litho Structurale des Formations Géologiques de la Presqu'île du Cap-Vert (Sénégal). Master's Thesis, Université Cheikh Anta Diop de Dakar, Dakar, Senegal, 2016; 65p.
62. Diombera, M. Territorial dynamics and tourism development: What sustainable environmental strategies in Saly (Petite Côte, Senegal)? *Études Caribéennes* **2020**, *6*, 18–24. [CrossRef]
63. Ndao, M. Dynamiques et Gestions Environnementales de 1970 à 2010 des Zones Humides au Sénégal: Étude de L'occupation du sol par Télédétection des Niayes avec Djiddah Thiaroye Kao (à Dakar), Mboro (à Thiès et Saint-Louis). Ph.D. Thesis, Université de Toulouse, Toulouse, France, 2012; 372p.
64. Diallo, S. Évolution Géomorphologique du Littoral sur la Petite Côte à Rufisque. Master's Thesis, Université Cheikh Anta Diop de Dakar, Dakar, Senegal, 1982; 117p.
65. Britannica. 2024. Available online: https://www.britannica.com/place/Senegal/Climate (accessed on 11 March 2024).

66. Capet, X.; Estrade, P.; Machu, E.; Ndoye, S.; Grelet, J.; Lazar, A.; Marié, L.; Dausse, D.; Brehmer, P. On the dynamics of the southern Senegal upwelling center: Observed variability from synoptic to superinertial scales. *J. Phys. Oceanogr.* **2017**, *47*, 155–180. [CrossRef]
67. Climatology. 2024. Available online: https://climateknowledgeportal.worldbank.org/country/senegal/climate-data-historical#:~:text=Two%20distinct%20seasons%20characterize%20Senegal%E2%80%99s,average%20of%201200%20mm/year (accessed on 11 March 2024).
68. Marti, F.; Cazenave, A.; Birol, F.; Passaro, M.; Léger, F.; Niño, F.; Almar, R.; Benveniste, J.; Legeais, J.F. Altimetry-based sea level trends along the coasts of western Africa. *Adv. Space Res.* **2021**, *68*, 504–522. [CrossRef]
69. Thoreux, C.; Sakho, I.; Sall, M.; Testut, L.; Wöppelmann, G. Trends in sea level around the Cap Vert peninsula, Senegal. *J. Coast. Res.* **2018**, *81*, 10–13.
70. Sarr CA, T.; Ndour MM, M.; Haddad, M.; Sakho, I. Estimation of Sea Level Rise on the West African Coasts: Case of Senegal, Mauritania and Cape Verde. *Int. J. Geosci.* **2021**, *12*, 121–137. [CrossRef]
71. Arabameri, A.; Pradhan, B.; Rezaei, K.; Conoscenti, C. Gully erosion susceptibility mapping using GIS-based multi-criteria decision analysis techniques. *Catena* **2019**, *180*, 282–297. [CrossRef]
72. Tadesse, T.B.; Tefera, S.A. Comparing potential risk of soil erosion using RUSLE and MCDA techniques in Central Ethiopia. *Model. Earth Syst. Environ.* **2021**, *7*, 1713–1725. [CrossRef]
73. Bagheri, M.; Zaiton Ibrahim, Z.; Mansor, S.; Abd Manaf, L.; Akhir, M.F.; Talaat WI, A.W.; Beiranvand Pour, A. Application of multi-criteria decision-making model and expert choice software for coastal city vulnerability evaluation. *Urban Sci.* **2021**, *5*, 84. [CrossRef]
74. Teshome, A.; Halefom, A. Mapping of soil erosion hotspot areas using GIS based-MCDA techniques in South Gondar Zone, Amhara Region, Ethiopia. *World News Nat. Sci.* **2019**, *24*, 218–238.
75. Taripanah, F.; Ranjbar, A.; Vali, A.; Mokarram, M. Classification of landforms using topographic location index and assessment of their actual Soil Erosion Risk in mountainous areas (Case study: Kharestan watershed). *Iran. J. Remote Sens. GIS* **2022**, *15*, 17–36. [CrossRef]
76. Dos Santos, J.C.; Lyra, G.B.; Abreu, M.C.; de Oliveira-Júnior, J.F.; Bohn, L.; Cunha-Zeri, G.; Zeri, M. Aridity indices to assess desertification susceptibility: A methodological approach using gridded climate data and cartographic modeling. *Nat. Hazards* **2022**, *111*, 2531–2558. [CrossRef]
77. CGIARCSI, 2024: Global Aridity and PET Database. Available online: https://csidotinfo.wordpress.com/data/global-aridity-and-pet-database/ (accessed on 2 February 2024).
78. Singh, O.; Singh, J. Soil erosion susceptibility assessment of the lower Himachal Himalayan Watershed. *J. Geol. Soc. India* **2018**, *92*, 157–165. [CrossRef]
79. WorldClim, 2024. Global Climate and Weather Data. Available online: https://www.worldclim.org/data/index.html#google_vignette (accessed on 2 February 2024).
80. Zwoliński, Z.; Jasiewicz, J.; Mazurek, M.; Hildebrandt-Radke, I.; Makohonienko, M. Geohazards and Geomorphological Setting in Poznań Urban Area, Poland. *J. Maps* **2021**, *17*, 202–214. [CrossRef]
81. Mortlock, T.R.; Goodwin, I.D.; McAneney, J.K.; Roche, K. The June 2016 Australian East Coast Low: Importance of wave direction for coastal erosion assessment. *Water* **2017**, *9*, 121. [CrossRef]
82. Schweiger, C.; Koldrack, N.; Kaehler, C.; Schuettrumpf, H. Influence of nearshore bathymetry changes on the numerical modelling of dune erosion. *J. Coast. Res.* **2020**, *36*, 545–558. [CrossRef]
83. GEBCO, 2023. Gridded Bathymetry Data. Available online: https://www.gebco.net/data_and_products/gridded_bathymetry_data/ (accessed on 2 February 2024).
84. Jarmalavičius, D.; Šmatas, V.; Stankūnavičius, G.; Pupienis, D.; Žilinskas, G. Factors controlling coastal erosion during storm events. *J. Coast. Res.* **2016**, *75*, 1112–1116. [CrossRef]
85. GlobalWindAtlas. 2024. Available online: https://globalwindatlas.info/en/ (accessed on 2 February 2024).
86. Copernicus Data Marine. Available online: https://data.marine.copernicus.eu/product/GLOBAL_MULTIYEAR_WAV_001_032/download (accessed on 10 March 2024).
87. Ahmed, N.; Howlader, N.; Hoque MA, A.; Pradhan, B. Coastal erosion vulnerability assessment along the eastern coast of Bangladesh using geospatial techniques. *Ocean Coast. Manag.* **2021**, *199*, 105408. [CrossRef]
88. Mani Murali, R.; Ankita, M.; Amrita, S.; Vethamony, P. Coastal vulnerability assessment of Puducherry coast, India, using the analytical hierarchical process. *Nat. Hazards Earth Syst. Sci.* **2013**, *13*, 3291–3311. [CrossRef]
89. Bondarenko, M.; Kerr, D.; Sorichetta, A.; Tatem, A.J. *Census/Projection-Disaggregated Gridded Population Datasets, Adjusted to Match the Corresponding UNPD 2020 Estimates, for 51 Countries across Sub-Saharan Africa Using Building Footprints. WorldPop*; University of Southampton: Southampton, UK, 2020. [CrossRef]
90. Geofabrik. Available online: https://download.geofabrik.de/africa.html (accessed on 19 February 2024).
91. Karuppusamy, B.; George, S.L.; Anusuya, K.; Venkatesh, R.; Thilagaraj, P.; Gnanappazham, L.; Kumaraswamy, K.; Balasundareshwaran, A.H.; Nina, P.B. Revealing the socio-economic vulnerability and multi-hazard risks at micro-administrative units in the coastal plains of Tamil Nadu, India. *Geomat. Nat. Hazards Risk* **2021**, *12*, 605–630. [CrossRef]
92. Riegel, C. *Risk Assessment and Critical Infrastructure Protection in Health Care Facilities: Reducing Social Vulnerability*; German Federal Service of Interior: Berlin, Germany, 2008.

93. Barzehkar, M.; Parnell, K.E.; Soomere, T.; Dragovich, D.; Engström, J. Decision support tools, systems and indices for sustainable coastal planning and management: A review. *Ocean Coast. Manag.* **2021**, *212*, 105813. [CrossRef]
94. Maanan, M.; Maanan, M.; Rueff, H.; Adouk, N.; Zourarah, B.; Rhinane, H. Assess the human and environmental vulnerability for coastal hazard by using a multi-criteria decision analysis. *Hum. Ecol. Risk Assess. Int. J.* **2018**, *24*, 1642–1658. [CrossRef]
95. ESA WorldCover Data. 2021. Available online: https://worldcover2021.esa.int/ (accessed on 19 February 2024).
96. Slocum, T.A.; McMaster, R.B.; Kessler, F.C.; Howard, H.H. *Thematic Cartography and Geovisualization*; CRC Press: Boca Raton, FL, USA, 2022. [CrossRef]
97. Saaty, T.L. Decision making with the analytic hierarchy process. *Int. J. Serv. Sci.* **2008**, *1*, 83–98. [CrossRef]
98. Guerin, K. Dynamics of the Sandy Coastline from Thiaroye to Bargny (Bay of Gorée Senegal). Master's Thesis, University of Paris 1-Sorbonne-Panthéon, Paris, France, 2003; p. 198.
99. Bakhoum, P.W.; Ndour, A.; Niang, I.; Sambou, B.; Traore, V.B.; Diaw, A.T.; Ndiaye, M.L. Coastline mobility of Goree Island (Senegal), from 1942 to 2011. *Mar. Sci.* **2017**, *7*, 1–9.
100. Sagne, P.; Ba, K.; Fall, B.; Youm JP, M.; Faye, G.; Sarr JP, G.; Sow, E.H. Cartography of the Historical Dynamics of the Coastline of the Beaches of Guédiawaye and Malika (Dakar, Senegal). *Eur. Sci. J.* **2021**, *17*, 214. [CrossRef]
101. Taveneau, A.; Almar, R.; Bergsma, E.W.; Sy, B.A.; Ndour, A.; Sadio, M.; Garlan, T. Observing and predicting coastal erosion at the Langue de Barbarie sand spit around Saint Louis (Senegal, West Africa) through satellite-derived digital elevation model and shoreline. *Remote Sens.* **2021**, *13*, 2454. [CrossRef]
102. Sadio, M.; Sakho, I.; Seujip, M.S.; Gueye, A.; Diouf, M.B.; Deloffre, J. Multi-decadal dynamics of the Saloum River delta mouth in climate change context. *J. Afr. Earth Sci.* **2022**, *187*, 104451. [CrossRef]
103. Enríquez-de-Salamanca, Á. Evolution of coastal erosion in Palmarin (Senegal). *J. Coast. Conserv.* **2020**, *24*, 25. [CrossRef]
104. Koulibaly, C.T.; Ayoade, J.O. The application of GIS and remote sensing in a spatiotemporal analysis of coastline retreat in Rufisque, Senegal. *Geomat. Environ. Eng.* **2021**, *15*, 55–80. [CrossRef]
105. Bossis, R. Quantifying Long-Term Coastal Erosion: Topographic Reconstruction of Volcanic Islands and Measurements of Cosmogenic Isotope Abundance in Coastal Cliff Colluviums. Ph.D. Thesis, University Paul Sabatier-Toulouse III, Toulouse, France, 2023. [CrossRef]
106. Pouye, I.; Adjoussi, D.P.; Ndione, J.A.; Sall, A. Evaluation of the Economic Impact of Coastal Erosion in Dakar Region. *J. Coast. Res.* **2024**, *40*, 193–209. [CrossRef]
107. Ndiaye, M. Dynamics, Socio-Economic Vulnerability and Governance of the Coastlines of Saly Portudal (Mbour) and Langue de Barbarie (Saint-Louis). Ph.D. Thesis, Université Gaston Berger de Saint Louis, Saint Louis, Senegal, 2016; 339p.
108. Coly, A.; Dieme, B. Ètude sur la vulnérabilité du secteur touristique à Saly et de ses implications socioéconomiques sur l'économie locale au niveau de la station touristique. In *Provisional Final Report*; Ministere de l'Environnement et de la Protection de la Nature: Berlin, Germnay, 2011; 40p. [CrossRef]
109. Fall, P.S. Analyzes Spatial Dynamics, Vulnerability and Adaptation Strategies of Populations Faced with Coastal Erosion: The Case of Popenguine-Ndayane (Petite Côte). Master's Thesis, Assane Seck University, Ziguinchor, Senegal, 2021; 106p.
110. Mar, A.S.; et Bell, J.M. Stratégies d'Adaptation Du Secteur Touristique De La Petite Côte Sénégalaise Face Aux Effets Du Changement Climatique. *Int. J. Progress. Sci. Technol.* **2022**, *34*, 37–48. [CrossRef]
111. Sidibe, I. A coastal territory in a political, economic and religious space in Senegal: The case of ouakam bay (Dakar). *Spaces Popul. Soc.* **2013**, 159–176. [CrossRef]
112. Sy, B.A. L'ouverture de la brèche de la Langue de Barbarie et ses conséquences, Approche géomorphologique. *Rech. Afr.* **2015**, *5*. Available online: https://revues.ml/index.php/recherches/article/view/802 (accessed on 27 July 2024).
113. Weissenberger, S.; Noblet, M.; Plante, S.; Chouinard, O.; Guillemot, J.; Aube, M. Climate change, coastal development and vulnerability: A comparison of French, Canadian and Senegalese territories. *VertigO—Electron. J. Environ. Sci.* **2016**, *16*, 2–33. [CrossRef]
114. Sy, A.A. Sedimentary Dynamics and Current Risks in the Saint-Louis-Gandiol Axis. Ph.D. Thesis, Gaston Berger University (UGB), Saint-Louis, Senegal, 2013; 333p.
115. Sy, B.A.; Bilbao, I.A.; Sy, A.A.; Perez, I.S.; Valido, S.R. Results of the 2010-2012 monitoring of the evolution of the breach opened on the Langue de Barbarie in Senegal and its consequences. *Phys. Geogr. Environ.* **2013**, *7*, 223–242. [CrossRef]
116. Sarr, M.A.; Pouye, I.; Sene, A.; Aniel-Quiroga, I.; Diouf, A.A.; Samb, F.; Ndiaye, M.L.; Sall, M. Monitoring and Forecasting of Coastal Erosion in the Context of Climate Change in Saint Louis (Senegal). *Geographies* **2024**, *4*, 287–303. [CrossRef]
117. Kane, C. Prevalence of the vulnerability to coastal erosion: Case study of Saint-Louis city. *Egypt. J. Environ. Chang.* **2023**, *15*, 179–190.
118. Rey, T.; Fanget, C. Inadequacy between coastal temporalities and decision and action times in Senegal: The example of the Brèche de Barbarie. *Territ. D'afrique* **2017**, *9*, 5–15.
119. Brüning, L. Typology of the consequences of migration on strategies for adapting to coastal erosion in Senegal. *Population* **2021**, *76*, 519–544. [CrossRef]
120. Barry, M.; Dièye, E.H.B.; Sané, T.; Sy, O.; Solly, B. Dynamics of the coastline in the commune of Kafountine (Lower Casamance). In Conference Vulnerability of coastal and estuarine societies and environments in West Africa. In Proceedings of the LMI-PATEO-UASZ International Colloquium, Assane Seck University, Ziguinchor, Senegal, 19–22 November 2019.

121. Thior, M.; Sy, A.A.; Cisse, I.; Dieye, E.H.B.; Sane, T.; Ba, B.D.; Solly, B.; Descroix, L. Cartographic approach to the evolution of the coastline in the Casamance estuary. Mappemonde. *Q. J. Geogr. Images Landf.* **2021**, *131*. [CrossRef]
122. Sané, T.; Dièye, E.H.B.; Solly, B.; Ba, B.D.; Thior, M.; Descroix, L.; Diakhaté, M.M. Vulnerability and resilience of coastal socio-ecosystems in West Africa: Current state of knowledge and questions about the future of the Senegal-Bissau-Guinea coast. Belgeo. *Rev. Belg. De Géographie* **2021**, *1*. [CrossRef]
123. Bocoum, S. Tourisme balnéaire face aux contraintes liées à l'érosion côtière en Basse Casamance (Sénégal): Cas de la commune de Kafountine. *Études Caribéennes* **2024**, 57–58. [CrossRef]
124. Descroix, L.; Dacosta, H.; Sané, T.; Cormier-Salem, M.C.; Bodian, A. Overview of the consequences of climate change through the rise in sea level: Coastal erosion and salinisation of water and soil. Water and Society in the Face of Climate Change in the Casamance Basin. In Proceedings of the Scientific Workshop and Launch of the Initiative 'Casamance: A Scientific Network at the Eservice of Development in Casamance, Ziguinchor, Senegal, 15–17 June 2015; pp. 75–89.
125. Barry, M. Coastal Erosion and Impacts in the Commune of Kafountine (Lower Casamance). Master's Thesis, Environment and Development Speciality, Assane Seck University, Ziguinchor, Senegal, 2016; 123p.
126. Diatta, L.S. Impacts of coastal dynamics between Cabrousse and Boudiédième (Commune of Djembéring) Lower Casamance. *Gegraphical Space Rev. Moroc. Soc.* **2020**, *58*, 173–198.
127. Thior, M.; Sané, T.; Abou Sy, A.; Barry, B.; Descroix, L. Morphological evolution of the sandy barrier of the bird peninsula on the Casamance coast (Senegal). *Rev. Marocaine De Géomorphologie* **2020**, *4*, 2020.
128. Sakho, I.; Sadio, M.; Camara, I.; Noblet, M.; Seck, A.; Saengsupavanich, C.; Ndour, A.; Diouf, M.B. Sea level rise and future shoreline changes along the sandy coast of Saloum Delta, Senegal. *Arab. J. Geosci.* **2022**, *15*, 1547. [CrossRef]
129. Sane, M.; Yamagishi, H. Coastal erosion in Dakar, western Senegal. *J. Jpn. Soc. Eng. Geol.* **2004**, *44*, 360–366. [CrossRef]
130. Narra, P.; Coelho, C.; Sancho, F.; Escudero, M.; Silva, R. Coastal hazard assessments for sandy coasts: Appraisal of five methodologies. *J. Coast. Res.* **2019**, *35*, 574–589. [CrossRef]
131. Croitoru, L.; Miranda, J.J.; Sarra, M. The cost of coastal zone degradation in West Africa: Benin, Cote d'Ivoire, Senegal and Togo. In *West African Coastal Area Management Programme (WACA)*; The World Bank: Washington, DC, USA, 2019.
132. Jevrejeva, S.; Williams, J.; Vousdoukas, M.I.; Jackson, L.P. Future sea level rise dominates changes in worst case extreme sea levels along the global coastline by 2100. *Environ. Res. Lett.* **2023**, *18*, 024037. [CrossRef]
133. Kopp, R.E.; Garner, G.G.; Hermans, T.H.J.; Jha, S.; Kumar, P.; Reedy, A.; Slangen, A.B.A.; Turilli, M.; Edwards, T.L.; Gregory, J.M.; et al. The Framework for Assessing Changes to Sea-level (FACTS) v1.0: A platform for characterizing parametric and structural uncertainty in future global, relative, and extreme sea-level change. *Geosci. Model Dev.* **2023**, *16*, 7461–7489. [CrossRef]
134. Yin, J. Rapid decadal acceleration of sea level rise along the US East and Gulf coasts during 2010–2022 and its impact on hurricane-induced storm surge. *J. Clim.* **2023**, *36*, 4511–4529. [CrossRef]
135. Woodroffe, C.D. Critical thresholds and the vulnerability of Australian tropical coastal ecosystems to the impacts of climate change. *J. Coast. Res.* **2024**, *50* (Suppl. S1), 464–468. [CrossRef]
136. Cazenave, A.; Cozannet, G.L. Sea level rise and its coastal impacts. *Earth's Future* **2014**, *2*, 15–34. [CrossRef]
137. Melet, A.; Meyssignac, B.; Almar, R.; Le Cozannet, G. Under-estimated wave contribution to coastal sea-level rise. *Nat. Clim. Chang.* **2018**, *8*, 234–239. [CrossRef]
138. Sahin, O.; Stewart, R.A.; Faivre, G.; Ware, D.; Tomlinson, R.; Mackey, B. Spatial Bayesian Network for predicting sea level rise induced coastal erosion in a small Pacific Island. *J. Environ. Manag.* **2019**, *238*, 341–351. [CrossRef]
139. Becker, M.; Karpytchev, M.; Hu, A. Increased exposure of coastal cities to sea-level rise due to internal climate variability. *Nat. Clim. Chang.* **2023**, *13*, 367–374. [CrossRef]
140. Boumis, G.; Moftakhari, H.R.; Moradkhani, H. Coevolution of extreme sea levels and sea-level rise under global warming. *Earth's Future* **2023**, *11*, e2023EF003649. [CrossRef]
141. Hirschfeld, D.; Behar, D.; Nicholls, R.J.; Cahill, N.; James, T.; Horton, B.P.; Portman, M.E.; Bell, R.; Campo, M.; Esteban, M.; et al. Global survey shows planners use widely varying sea-level rise projections for coastal adaptation. *Commun. Earth Environ.* **2023**, *4*, 102. [CrossRef]
142. Ohenhen, L.O.; Shirzaei, M.; Ojha, C.; Kirwan, M.L. Hidden vulnerability of US Atlantic coast to sea-level rise due to vertical land motion. *Nat. Commun.* **2023**, *14*, 2038. [CrossRef] [PubMed]
143. Vecchio, A.; Anzidei, M.; Serpelloni, E. Sea level rise projections up to 2150 in the northern Mediterranean coasts. *Environ. Res. Lett.* **2024**, *19*, 014050. [CrossRef]